NUREG/CR-6816
ANL-02/36

Review and Assessment of Codes and Procedures for HTGR Components

Argonne National Laboratory

U.S. Nuclear Regulatory Commission
Office of Nuclear Regulatory Research
Washington, DC 20555-0001

NUREG/CR-6816
ANL-02/36

Review and Assessment of Codes and Procedures for HTGR Components

Manuscript Completed: February 2003
Date Published: June 2003

Prepared by
V. N. Shah, S. Majumdar,
K. Natesan

Argonne National Laboratory
9700 South Cass Avenue
Argonne, IL 60439

C. A. Greene, NRC Project Manager

Prepared for
Division of Engineering Technology
Office of Nuclear Regulatory Research
U.S. Nuclear Regulatory Commission
Washington, DC 20555-0001
NRC Job Code Y6537

Review and Assessment of Codes and Procedures for HTGR Components

by

V. N. Shah, S. Majumdar, and K. Natesan

Abstract

The report reviews and evaluates currently available national and international codes and procedures for use in the design of high-temperature gas-cooled reactors (HTGRs) including, but not limited to, the Gas Turbine-Modular Helium Reactor (GT-MHR) and the Pebble Bed Modular Reactor (PMBR). It includes an evaluation of the applicability of the codes, standards, and procedures to the materials that have been used or recommended for HTGRs, taking into account the HTGR operating temperature and environments. Seven codes and procedures, including five ASME Codes and Code Cases, one French Code (RCC-MR), and one British Procedure, were reviewed and evaluated. The ASME Codes and Code Cases included Section III, Subsection NB and Subsection NH; Code Cases N-499-1, N-201-4; and the draft Code Case for Alloy 617. Major findings of the evaluation are the following. (1) Most of the materials needed for HTGR are not included in the code cases. New code cases are needed for these materials. (2) The maximum temperature permitted by the codes and code cases for the materials acceptable for HTGR components is lower (760°C) than the maximum temperature (850°C or higher) that these components may experience in reactor service. The scope of the code and code cases needs to be expanded to include materials with allowable temperatures of ≥850°C. (3) The codes and code cases do not provide specific guidelines for environmental effects, especially the effect of impure helium, on the high temperature behavior (e.g., creep and creep-fatigue) of the materials considered. The needed data on environmental effects should be collected or generated, if not available, so that the specific guidelines for these effects can be developed. Although the linear damage rule has been adopted by many design codes for estimating creep-fatigue damage, other potentially superior predictive models need to be evaluated and further developed for HTGR components operating under helium environment. The linear damage rule is not a good description of behavior if environmental effects (e.g., surface cracking) play an important role in high temperature fatigue. Life predictive models for surface cracking have to be developed for this type of damage.

Contents

Abstract iii

Executive Summary ix

Acknowledgments xv

1 Introduction 1

2 Operating Environment and Candidate Materials for Selected HTGR Plants 3

3 ASME Design Codes 8

3.1 Historical Background 8

3.2 Basic ASME Code Definitions 9

3.2.1 Loading Categories 9

3.2.2 Classification of Stresses 10

3.3 ASME B&PV Code, Section III, Subsection NB 11

3.3.1 Limits for Primary Stress 11

3.3.2 Low-Temperature Limits for Cyclic Loading 14

3.3.3 Low-Temperature Ratcheting Limits 14

3.3.4 Low-Temperature Fatigue Limits 15

3.3.5 Low-Temperature Fast Fracture 17

3.3.6 Buckling Limits 17

3.4 ASME B&PV Code, Section III, Subsection NH 17

3.4.1 High-Temperature Design Rules 18

3.4.2 Material Properties Database Needed 18

3.4.3 Primary Stress Limits 19

3.4.4 High-Temperature Limits for Cyclic Loading 22

3.4.5 High-Temperature Ratcheting Limits 23

3.4.6 High-Temperature Creep-Fatigue Rule 27

3.4.7 Creep Crack Growth and Nonductile Fracture 29

3.4.8 Time-Independent Buckling 30

3.4.9 Time-Dependent Buckling 30

3.4.10 Evaluation of Subsection NH 30

3.5 ASME B&PV Code Case N-499-1 32

3.5.1 Summary of Code Case N-499-1 32

3.5.2 Evaluation of Code Case N-499-1 34

3.6 ASME B&PV Code Case N-201-4 34

3.6.1 Summary of Code Case N-201-4 34

3.6.2 Evaluation of Code Case N-201-4 36
3.7 ASME B&PV Draft Code Case for Alloy 617 37
3.7.1 Draft Code Case Features 37
3.7.2 Allowable Stress and Stress Rupture Values 38
3.7.3 Unified Constitutive Model and Isochronous Stress-Strain Curves 40
3.7.4 High-Temperature Limits for Cyclic Loading 42
3.7.5 High-Temperature Ratcheting Limits 44
3.7.6 High-Temperature Creep-Fatigue Rule 44
3.7.7 Buckling Rules 44
3.7.8 Evaluation of the Draft Code Case 45
4 RCC-MR, Design and Construction Rules for Mechanical Components of FBR Nuclear Islands (French Code) 46
4.1 Background Information on Efficiency Diagram 48
4.2 Comparison between Efficiency Diagram and the Bree Diagram 48
4.3 Evaluation of Code RCC-MR 49
5 Procedure R5, Assessment Procedure for the High-Temperature Response of Structures 51
5.1 Creep Crack Growth Assessment 51
5.2 Creep-Fatigue Evaluation 52
5.3 Evaluation of the R5 Procedure 52
6 Predictive Rules for Creep, Fatigue, and Creep-Fatigue Damage 54
6.1 "Safety Factors" Two and Twenty on Fatigue Life in Air 54
6.2 Predictive Rules for Creep Damage 54
6.3 Predictive Rules for Fatigue Damage at High Temperature 55
7 Findings 58
References 60

Figures

2.1 Schematic of gas turbine-modular helium reactor 5

3.1 Bree diagram for axisymmetric shell under steady internal pressure and cyclic thermal stress due to linear through-thickness temperature gradient..... 15

3.2a Classical creep curve 20

3.2b Nonclassical creep curve..... 20

3.3 Variation of high-temperature effective bending shape factor K_t for creep with Norton creep exponent..... 22

3.4 Effective creep stress parameter Z for simplified inelastic analysis rules B1 and B3 26

3.5 Creep-fatigue damage envelope for both elastic and inelastic analysis rules 27

3.6 Design fatigue strain range for SA-533B Class 1 and SA-508 Class 3 33

3.7 Isochronous stress-strain curves for low-alloy steels for 538°C..... 33

3.8 S_m and S_t for given times vs temperature for Alloy 617..... 39

3.9 S_t vs time for given temperature for Alloy 617..... 40

3.10 S_r vs time for given temperature for Alloy 617 40

3.11 Calculated and observed stress vs strain for Alloy 617 at 750°C for given strain rates..... 40

3.12 Calculated and observed stress vs strain for Alloy 617 at 950°C for given strain rates..... 41

3.13 Calculated and observed strain vs time for Alloy 617 at 950°C for given stresses..... 41

3.14 Average isochronous stress vs strain for Alloy 617 at 649°C at given times 42

3.15 Average isochronous stress vs strain for Alloy 617 at 982°C for given times 42

3.16 Design fatigue strain, ε_t, for Alloy 617..... 44

4.1 Comparison of the RCC-MR efficiency diagram with those calculated from Bree diagram analyses..... 49

Tables

2.1 Characteristics of selected steam cycle HTGRs 3

2.2 Characteristics of selected modular HTGR gas turbine plants 4

2.3 GT-MHR component materials 6

3.1 Maximum allowable temperatures for the materials included in Subsection NH 18

3.2 Maximum allowable temperatures for the materials included in Code Case N-201-4 .. 34

Executive Summary

The objective of the task is to review and evaluate currently available national and international codes and procedures to be used in design of high-temperature gas-cooled reactors (HTGRs) including, but not limited to, the Pebble Bed Modular Reactor (PBR) and the Gas Turbine-Modular Helium Reactor (GT-MHR) designs. The approach includes evaluation of the applicability of the codes, standards, and procedures to the materials that have been used or recommended for HTGRs, taking into account the HTGR operating environments. A companion report addresses the material database and coolant effects on materials pertinent to HTGR components (Natesan et al. 2003). The present report reviews the following codes, code cases, and procedure:

ASME B&PV Code, Section III, Subsection NB, Class 1 Components,

ASME B&PV Code, Section III, Subsection NH, Class 1 Components in Elevated Temperature Service,

ASME B&PV Code Case N-499-1, Use of SA-533 Grade B, Class 1 Plate and SA-508 Class 3 Forgings and Their Weldments for Limited Elevated Temperature Service,

ASME B&PV Code Case N-201-4, Class CS Components in Elevated Temperature Service,

Draft ASME B&PV Code Case for Alloy 617 (was being developed by the Task Group on Very-High Temperature Design),

RCC-MR, Design and Construction Rules for Mechanical Components of FBR Nuclear Islands (French Code), and

Procedure R5, Assessment Procedures for the High Temperature Response of Structures (British Procedure).

Major findings of the evaluation are as follows:

(1) Most of the materials needed for HTGR are not included in the code cases. New code cases are needed for these materials.

(2) The maximum temperature permitted by the codes and code cases for the materials acceptable for HTGR components is lower (760°C) than the maximum temperature (≥850°C) that these components may experience during operation. The scope of the code and code cases needs to be expanded to include the materials with allowable temperatures of 850°C and higher.

(3) The codes and code cases do not provide specific guidelines for environmental effects, especially the effect of impure helium on the high temperature behavior (e.g., fatigue, creep, and creep-fatigue) of the materials considered. High-temperature fatigue life may be influenced more by environment than by creep damage for some materials. Carburization or decarburization in impure gaseous He environment may have an effect on high temperature fatigue life. This phenomenon needs to be explored by tests and the effects incorporated in a life predictive model.

The in-depth evaluation of these codes, code cases, and procedure is as follows.

ASME Code, Subsection NB

The ASME Boiler and Pressure Vessel Code (ASME B&PV Code) Subsection NB of Section III of the Code provides design rules for Class 1 components at relatively low temperature [≤371°C (≤700°F)] for ferritic steels and ≤427°C (≤800°F) for austenitic stainless steels and high-nickel alloys. The design of HTGR components needs to satisfy these low-temperature design rules in addition to the high-temperature design rules discussed below.

ASME Code, Subsection NH

Subsection NH provides the high temperature design rules for out-of-core nuclear structures. The rules were developed in support of the U.S. liquid metal fast breeder reactor (LMFBR) program. Therefore, the available material choice is limited to five candidates – Types 304 and 316 austenitic stainless steels (up to 816°C), 2.25Cr-1Mo steel (up to 593°C), Alloy 800H (up to 760°C) for applications other than bolt, and Alloy 718 (up to 566°C) for bolt. In addition to providing design rules to protect against low temperature damages such as plastic collapse, plastic instability, buckling, cyclic ratcheting, and fatigue, Subsection NH also provides design rules to account for potential high temperature damages such as creep rupture, excessive creep deformation, creep buckling, cyclic creep ratcheting, and creep fatigue. Except for ferritic steels, which exhibit ductile-to-brittle transition behavior, the code does not require design to protect against brittle fracture using fracture mechanics analysis. In view of the high ductility and toughness of the permissible materials, this is reasonable. The creep-fatigue evaluation procedure does not account for environment effects, and the use of the bilinear creep and fatigue damage summation rule may not be universally applicable to all materials. Design rules were developed by the ASME Section III code committees on a consensus basis, and for the most part, these are followed by other countries as well. The two main difficulties of using Subsection NH to the design of HTGRs are the rather limited choice of materials, and the code allowable temperatures are not sufficiently high for HTGR application. To expand the material choice for HTGR applications, high-temperature design data for other potential candidates, including their weldments, have to be generated. A companion report on materials addresses several of these issues (Natesan et al. 2002). Therefore, the scope of this code needs to be expanded to include the materials with allowable temperature ≥850°C.

ASME Code Case N-499-1

Code Case N-499-1 may be applicable to GT-MHR reactor pressure vessel and connecting pipe made of low-alloy steels (SA 508 Cl 1, SA 533 Gr B, Cl 1) with a normal operating temperature of 290°C, provided the requirements on allowable cumulative time and maximum temperature for upset, emergency, and faulted conditions are satisfied. The normal operating temperature requirement is satisfied, if the vessel is insulated or cooled by helium returning from the turbine. The code case does not address the effect of the helium environment on these materials. The effect of helium environment (including impurities) on elevated-temperature (538°C) fatigue design curves, isochronous stress-strain curves, stress ruptures curves, and the creep-fatigue damage envelope needs to be evaluated to further assess the applicability of this code case to the low alloy steels used as pressure vessel materials.

ASME Code Case N-201-4

Code Case N-201-4 provides design rules for the construction of core support structures fabricated from five materials: ferritic steels 1 Cr-0.5 Mo-V and 2.25 Cr-1 Mo, Type 304 and 316 stainless steel (SS), and Alloy 800H. These rules are similar to those for Subsection NH. Some of these materials are not suitable for the high temperatures anticipated for core support structures in HTGRs. Ferritic steel, 1Cr-0.5Mo-V, is not suitable because the maximum allowable metal temperature is low (538°C), and its use is not permitted by Part B of the code case, which accounts for both creep and stress rupture effects. Austenitic stainless steels (Types 304 and 316 SS) have commonly been used for high-temperature steam application due to their excellent strength retention at high temperatures. However, a sufficient database is not available for the use of these alloys at temperatures of 600°C and higher in an impure helium environment of HTGRs. Furthermore, the austenitic stainless steels exhibit high thermal expansion rates and low thermal conductivity. This results in the development of high thermally induced stresses during heating and cooling, which can cause thermal fatigue and creep. Ferritic steel, 2.25 Cr–1 Mo, may be used for the reactor core support structures and internals located in the upper portion of the GT-MHR vessel, where the metal temperatures may be less than 500°C because of the low core inlet temperature of the coolant. Alloy 800H may be used to fabricate the support structures and internals that are exposed to the maximum temperature of 760°C.

The maximum temperature permitted by Code Case 201-4 for the materials acceptable for the HTGR core support structures is 760°C. Since the GT-MHR core support structures, especially those located in the lower portion of the reactor pressure vessel, may experience temperatures ≥ 850°C, the scope of the code case needs to be expanded to include the materials with higher allowable temperatures. The candidate materials for core support structures and vessel internals are Alloy 617 at high temperatures and 9Cr-1Mo-V steel for lower temperatures. A draft code case discussed later provides design rules for Alloy 617. Code RCC-MR provides design rules for 9Cr-1Mo-V steel. Code Case 201-4 does not provide specific guidelines for environmental effects, but states that the combined effects of exposure to elevated temperature, contacting fluid, and nuclear radiation on material properties shall also be considered. Therefore, the effects of helium coolant (with impurities) on the material properties need to be evaluated.

Draft ASME Code Case for Alloy 617

The draft code case for Alloy 617 provides design rules for very-high-temperature reactors (VHTRs) such as GT-MHR. VHTR reactor outlet temperatures of about 950°C are needed for some of the potential applications such as steam gasification of coal. The original request to the ASME Boiler and Pressure Vessel Code Committee for design rules for very-high-temperature nuclear components came from the U.S. Department of Energy (DOE) and one of its contractors. Materials of potential interest included nickel alloys 800H, Hastelloy X, and Alloy 617. An ad hoc task force of the ASME Code was established in 1983 to address the design of reactors operating at very high temperatures. The task force was organized under the jurisdiction of the Subgroup on Elevated Temperature Design of the Subcommittee on Design. The Task Force completed the draft code case in 1989 and submitted it to the Subgroup, which later approved the code case. No further work was done on the draft code case because of the lack of further interest from USDOE and its contractor.

The draft code case was patterned after relevant portions of Code Case N-47 and was limited to Alloy 617, temperature of 982°C (1800°F), and maximum service life [total life at temperatures >427°C (>800°F)] of 100,000 h or less. The draft code case focused on Alloy 617 because it was a leading candidate of designers, and there was a significant material properties database at the temperature of interest. The code case focused on all the failure modes that are addressed by Subsections NB and NH, including non-ductile failure. The last failure mode was considered because of the significant loss of fracture toughness in Alloy 617 after long-term exposure to high temperatures.

Most of the design rules provided by the draft code case are similar to those provided by Subsection NH. Some design rules are different from the Subsection NH rules because the draft code case considers higher temperature and different material. One of the main differences is that Alloy 617 exhibits unique behavior that includes (1) lack of clear distinction between time-independent and time-dependent behavior, (2) high dependence of flow stress on strain rate, and (3) softening with time, temperature, and strain. Therefore, design rules of Subsection NH that are time- and rate-independent, or strain hardening idealizations of material behavior, required careful consideration in the draft case. For example, the case specifies that inelastic design analyses for temperatures above 649°C (1200°F) must be based on unified constitutive equations, which do not distinguish between time-independent plasticity and time-dependent creep.

Extended exposure at elevated temperature may cause a significant reduction in fracture toughness of Alloy 617. The draft case requires a fracture mechanics analysis to justify the ability of the component to withstand the expected service conditions, especially when the component cools down to lower temperatures. Because of this concern for potential loss of fracture toughness, Alloy 617 bolting is excluded from the draft case. In addition, exposure of cold worked material to very high temperatures results in recrystallization. Therefore, cold worked Alloy 617 is also excluded from the draft case.

The draft code case is based on a limited database and minimal service experience. Further development of the draft code case is needed before the alloy could be satisfactorily and reliably applied. The recommendations for further development are presented below in three categories:

Actions Required to Complete the Draft Case

- Alloy 617 must be added to the low-temperature rules of Section III.
- Weldment stress rupture factors must be added.
- Thermal expansion coefficient must be added.
- Additional isochronous stress-strain curves at 427°C to 649°C must be added.

Material Data Needs

- Weldment fatigue data.
- More complete creep-fatigue database.
- The synergistic effects of aging, environment (including radiation), loading, and temperature.
- The effects of aging on toughness of materials.

Structural Design Methodology Needs

- Unified constitutive model are needed for developing isochronous stress-strain curves.
- Some very high-temperature, time-dependent tests of Alloy 617 structural models are needed to (1) provide better understanding of structural behavior and failure modes, and (2) validate inelastic analysis methods and failure modes.
- Simplified ratcheting evaluation procedures need to be developed for temperatures above 649°C.
- The use of linear damage fractions as the basis of the creep-fatigue rules is probably the biggest shortcoming of the draft case. A basic effort is needed to identify and experimentally validate a more fitting damage theory.

French Code RCC-MR

RCC-MR was developed in France as a high-temperature extension to RCC-M, for the French breeder reactor program. The basic rules in RCC-MR are similar to those in ASME Code Subsection NH. RCC-MR provides more detailed instructions for fatigue and creep-fatigue design analysis than given in the ASME Codes. It also uses a somewhat different approach for analysis of creep ratcheting without the use of isochronous stress-strain curves. But the basic safety factors used in the generation of design curves in the two codes are comparable. The choice of materials in RCC-MR is also limited.

British Procedure R5

Procedure R5 is a comprehensive assessment procedure for the high temperature response of structures. The procedure addresses several aspects of high temperature behavior, including creep and creep fatigue crack growth. The main objective of the procedure is to ensure that failure of both defect-free and defective components by creep rupture is avoided. The calculation of the expected lifetime is performed by conservative approximations based on Reference Stress Techniques. Procedure R5 permits use of ductility exhaustion for creep-fatigue evaluation, if the material data are available. If appropriate data are not available, linear damage summation, similar to that recommended by ASME Code Subsection NH, is used.

Procedure R5, which is a guideline and not a code, considers creep cracking explicitly. Neither the ASME Code nor the RCC-MR Code addresses the subject because creep cracking is more of an issue in residual life assessment than design. Therefore, the use of this procedure in the design of HTGR components is limited. However, the procedure presents the use of ductility exhaustion as an alternative to the linear damage rule for calculating the creep component of damage. The use of ductility exhaustion instead of linear damage rule may be more suitable for estimating creep damage in the HTGR materials and should be evaluated for incorporation in Subsection NH.

Life-Predictive Models for High Temperature Fatigue

The linear damage rule (D-diagram) approach, which is used by many design codes including the ASME Code, was originally developed from tests on austenitic stainless steels for which tensile creep damage (intergranular cavitation) rather than environmental effects plays a major role in determining creep-fatigue life. There are other life predictive models, such as

Damage Rate Equations, Strain Range Partitioning Equations, the Frequency Separation Equation, and the Ductility Exhaustion Equation, which are potentially more accurate than the linear damage rule and need to be explored for application to HTGR materials. Because of its simplicity of use, the linear damage rule has been force-fitted for other materials (e.g., ferritic steels) whose high-temperature fatigue life is influenced more by surface cracking (environmental effect) than by bulk creep damage. However, extrapolation beyond the database using linear damage rule cannot be justified. Specialized models for predicting surface cracking due to environmental effects need to be developed for such purposes. Carburization or decarburization in impure gaseous He environment may have an effect on high-temperature fatigue life. This phenomenon needs to be explored by tests and the effects incorporated into a life predictive model.

Acknowledgments

This work is sponsored by the Office of Nuclear Regulatory Research, U.S. Nuclear Regulatory Commission, under Job Code Y6537; Senior Technical Advisor: J. Muscara; Program Manager: C. A. Greene. The authors thank J. M. Corum for providing published papers and other documents related to draft ASME Code Case for Alloy 617. Figures 3.8 to 3.16 in the report are reprinted with permission from the American Mechanical Engineers Society, who is the original publisher of these figures. The sources for these figures and their authors are identified in the report along with the figures.

1 Introduction

The objective of this task is to review and evaluate currently available national and international codes, standards and procedures to be used in design and fabrication of high-temperature gas-cooled reactors (HTGRs) including, but not limited to, the Pebble Bed Modular Reactor (PBR) and the Gas Turbine-Modular Helium Reactor (GT-MHR) designs. The approach includes evaluation of the applicability of the codes, standards, and procedures to the materials that have been or to be used in HTGRs, taking into account the HTGR operating environments.

In the United States, components of nuclear reactor systems are designed in accordance with applicable provisions of the ASME Boiler and Pressure Vessel Code (ASME B&PV Code). Subsection NB of Section III of the Code provides design rules for Class 1 components at relatively low temperature [371°C (700°F) or lower for ferritic steels and 427°C (800°F) or lower for austenitic steels and high-nickel alloys]. Subsection NH of Section III of the Code provides design rules for Class 1 components at higher temperatures [593°C (1100°F) or lower for ferritic steel, 760°C (1400°F) or lower for high-nickel alloys, and 816°C (1500°F) or lower for austenitic steels]. Code Case N-499-1 provides design rules for Class 1 pressure vessels at higher temperatures, in the range of 371°C to 538°C, for limited time. Code Case N-201-4 provides design rules for core support structures, which are similar to those provided by Subsection NH. The draft code case for Alloy 617 provides design rules for Alloy 617 at very high temperature [982°C (1800°F) or lower]. These codes and code cases along with a French Code and a British Procedure, which are listed below, are reviewed in this report.

ASME B&PV Code, Section III, Subsection NB, Class 1 Components,

ASME B&PV Code, Section III, Subsection NH, Class 1 Components in Elevated Temperature Service,

ASME B&PV Code Case N-499-1, Use of SA-533 Grade B, Class 1 Plate and SA-508 Class 3 Forgings and Their Weldments for Limited Elevated Temperature Service,

ASME B&PV Code Case N-201-4, Class CS Components in Elevated Temperature Service,

Draft ASME B&PV Code Case for Alloy 617 (was being developed by the Task Group on Very-High Temperature Design),

RCC-MR, Design and Construction Rules for Mechanical Components of FBR Nuclear Islands (French Code),

Procedure R5, Assessment Procedures for the High Temperature Response of Structures (British Procedure).

The outline of this report is as follows. Chapter 2 identifies the operating environment and candidate structural materials for selected HTGR plants. The emphasis is on the gas turbine-modular helium reactor (GT-MHR). Chapter 3 presents a review and evaluation of several ASME Codes for their applicability to the design of components for high temperature service. Section 3.1 presents historical background of the ASME Design Code. Section 3.2

reviews the basic definitions for load categories and stress classification that are common to all the codes. Section 3.3 discusses the low temperature rules and procedures as provided in Subsection NB, and Section 3.4 does the same for the high-temperature design process as discussed in Subsection NH. Sections 3.5, 3.6, and 3.7 review ASME Code Cases N-499-1 and N-201-4, and the draft code case for Alloy 617, respectively. Sections 4 and 5 review the design procedures of the French Code RCC-MR and British Procedure R5, respectively. Section 6 summarizes the weaknesses in codes and procedures and presents recommendations for improvements to these codes and standards.

2 Operating Environment and Candidate Materials for Selected HTGR Plants

Several HTGR designs have been developed in different countries. These designs may be divided into two main groups: (1) steam-cycle HTGRs and (2) modular gas turbine HTGRs. Tables 2.1 and 2.2, respectively, present characteristics of selected steam-cycle HTGRs and modular gas turbine HTGRs. In all HTGR designs, helium serves as a primary coolant. In steam-cycle HTGRs, helium is used to produce steam, which, in turn, drives the turbines to generate power. In modular gas turbine HTGRs, helium is generally used to directly drive the turbines; but in two designs, as mentioned in Table 2.2, helium is used to heat either air or nitrogen, which drives the turbines. The characteristics listed in Tables 2.1 and 2.2 include the country of origin for a given design, thermal and net electric power, core type, core outlet temperature, helium pressure, secondary coolant, and vessel material. Several steam-cycle HTGRs had been in operation for some period, and their operation dates are listed in Table 2.1. The components are exposed to the maximum temperature in the range of 700 to 950°C. The vessel materials include either prestressed concrete or ferritic steels (e.g., SA 508, SA 516-70, SA 533, and Modified 9Cr-1Mo).

Table 2.1. Characteristics of selected steam cycle HTGRs
(Boyer et al. 1974, Brey 2000, Nickel 1989)

	AVR	Peach Bottom	Ft. St. Vrain	Fulton	THTR-300	HTR-500	VGM-400	HTR-Module	MHTGR
Country of Origin	Germany	U.S.	U.S.	U.S.	Germany	Germany	Russia	Germany	U.S.
Thermal Power, MWt	46	115	842	2,979	750	1,390	1,060	200	350
Net. Electric Power, MWe	13	40	330	1,160	300	550	Co-Gen.	80	139
Core Outlet Temp., °C	950	725	775	741	750	700	950	700	686
Helium Pressure, MPa	1.1	2.25	4.8	5.0	3.9	5.5	5.0	6.6	6.4
Steam Temp., °C	505	538	538/538	513	530/530	530	535	530	538
Reactor Type	Pebble	Sleeve	Block	Block	Pebble	Pebble	Pebble	Pebble	Block
Vessel Material	Steel	Steel	PCRV*	PCRV	PCRV	PCRV	PCRV	Steel	Steel
Date of Operation	1966	1967	1979 to 1989	No operation	1985	No operation	No Data	No operation	No operation

*Prestressed concrete reactor vessel.

Table 2.2. Characteristics of selected modular HTGR gas turbine plants* (Brey 2000)

	GT-MHR	PBMR	MHTGR-IGT	ACACIA	GTHTR-300	HTR-GT 600MW	MPBR
Country of Origin	U.S./Russia	S. Africa	China	Netherlands	Japan	Japan	U.S.
Thermal Power, MWt	600	265	200	40	600	600	250
Net. Electric Power, MWe	278	116	~96	Co-Gen.	273	287	112
Core Outlet Temp., °C	850	900	900	800	850	850	850
Helium Pressure, MPa	7.15	7.0	6.0	2.3	6.8	6.0	7.9
Cycle Type (Secondary Coolant)	Direct	Direct	Indirect (nitrogen gas)	Direct	Direct	Direct	Indirect (air)
Core Type	Block	Pebble	Pebble	Pebble	Block	Pin/Block	Pebble
Vessel Material	Mod 9Cr1Mo	SA 508	SA 516-70	Steel	SA 508	Mod 9Cr1Mo	Steel

*The systems were either planned or designed, but none were constructed.

The main focus of the report is on the applicability of the codes and standards to the materials for the Gas-Turbine-Modular Helium Reactor (GT-MHR), which is under preapplication review for certification and is shown in Fig. 2.1. Table 2.3 lists the GT-MHR component materials and the operating environments. The components are exposed to helium in the operating temperature range of ≈100 to 950°C. Helium gas is chemically inert, but reactor-grade helium contains traces of reactive impurities such as hydrogen, methane, oxygen, carbon monoxide, carbon dioxide, and water vapor. These impurities can oxidize and/or carburize/decarburize the structural components, which in turn can influence the mechanical properties.

The last column in Table 2.3 lists the ASME Codes and Code Cases that may be potentially used for designing HTGR components. Natesan et al. (2003) have identified some recently published data (post-1991 data) for the candidate materials at high temperatures and in an air environment. These data may be used to assess the capabilities of the listed codes and code cases. As discussed in the report, the scope of these codes and code cases needs to be enlarged and their capability enhanced so that they can be used in designing the GT-MHR components and the components of other HTGR designs. The enlarged scope should include the candidate materials identified by Natesan et al. (2003). Several of these materials are currently not included in the codes and code cases evaluated in the report. The enhanced capability should include development of predictive rules for creep, fatigue, and creep-fatigue behavior of the candidate materials at the high GT-MHR temperatures and in the helium environment, including impurities. Natesan et al. (2003) summarized the available material behavior data for the candidate materials at high temperatures and in helium environments. These data may be used for enhancing the codes and code cases evaluated in the report.

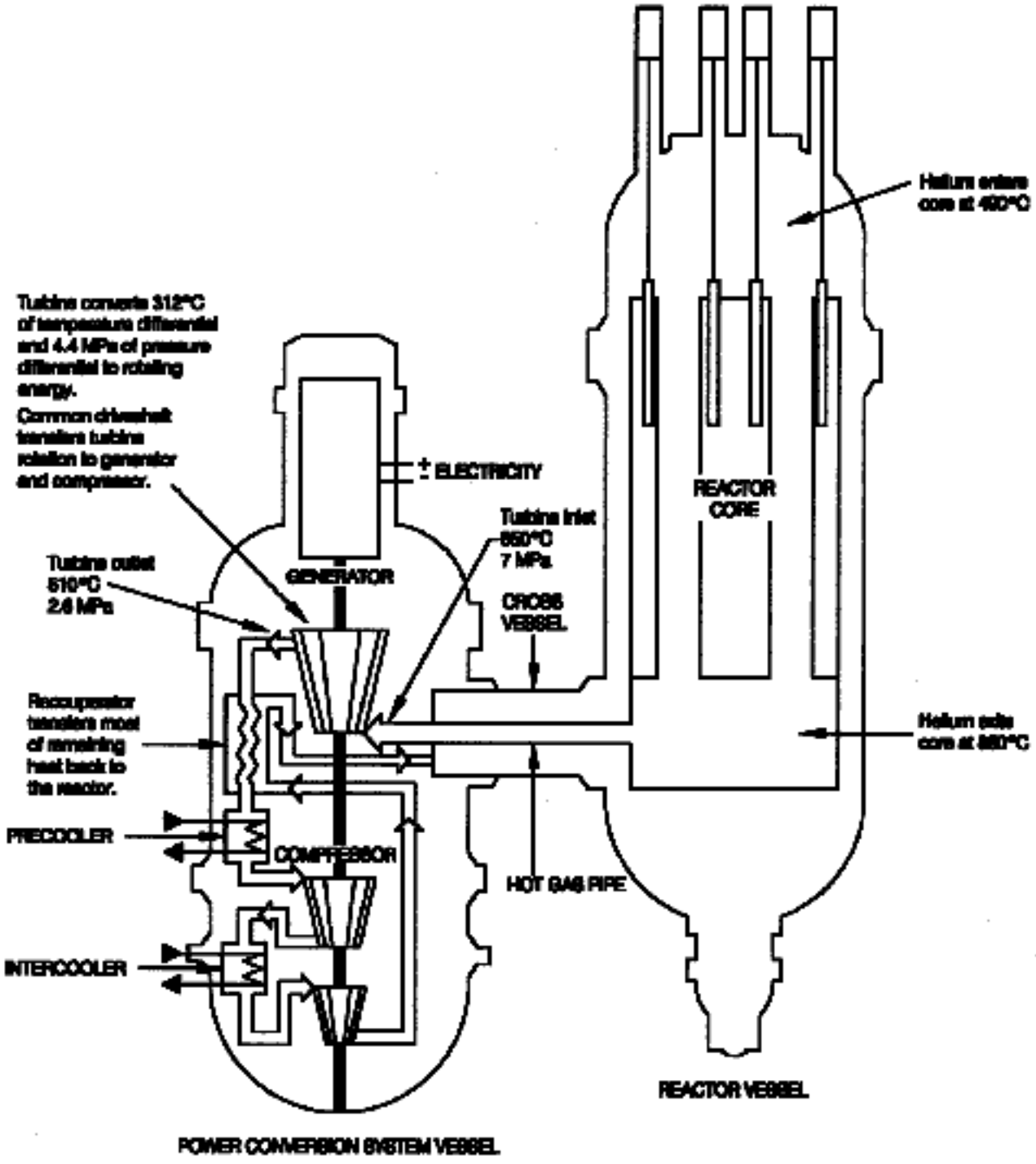

Figure 2.1. Schematic of gas turbine-modular helium reactor (GT-MHR)

Table 2.3. GT-MHR component materials

Components	Environment	Material	Comments	References	Code Status
Reactor Pressure Vessel Cross vessel	Normal operating temperature 290°C Pressure ~7.07 MPa	SA 508 GR3, Cl1 SA 508 Class 1 SA 533 Grade B, Class 1	Insulated vessel design or vessel cooled by helium returning from turbine	EPRI 2002 Shenoy and Betts 1988; Muto et al. 2000; Buckthorpe et al. 2002	ASME Code Case N-499-1
	Normal operating temperature ~ 500°C	9Cr-1Mo-V (Also called Modified 9Cr1Mo) (10X9MFB in Russia)	This material is not yet authorized as the Class 1 vessel material. Mod 9Cr1Mo has a big advantage over 2.25Cr1Mo above 450°C; limited data for as-received and post-weld heat-treated base material and weldments; limited fabrication experience. Tests scheduled to begin mid 2002.	Muto et al. 2000 IAEA 2001 Buckthorpe et al. 2002 Kiryushin et al. 1997	None available
Reactor System Metallic Components - core support structure - reactor internals	Core inlet/outlet temperatures 491/850°C	2-1/4 Cr-1 Mo Type 316 SS Alloy 800H Alloy 617 Hastelloy X	The support structure includes the upper support plate, core barrel shell, gas duct shell, bottom collector header shroud, hot duct nozzle, and the shutdown cooling system header. The reactor internals include top collector plenum and its shroud, hot duct assembly, control rod canister, plenum element casing, and core lateral restraint.	LaBar 2002; Shenoy and Betts 1988 EPRI 2002 IAEA 2001 Natesan et al. 2003	ASME Code Case N-201-4 (Maximum allowable temperatures of 816°C or lower – See Table 5) ASME Draft Code Case for Alloy 617 (Maximum allowable temperature of 982°C)
Shutdown Cooling System (SCS) - conical shell - bottom - gas circulator	850°C (conical shell) 490°C (bottom and gas circulator)	Alloy CrNi55MoWZr (conical shell) Type 321 SS (gas circulator blades)		EPRI 2002	None available
Reactor Core Cooling System (RCCS) Component	490°C	Type 321 SS		EPRI 2002	None available

Table 2.3. GT-MHR component materials (continued)

Components	Environment	Material	Comments	References	Code Status
Hot Gas Pipe	850°C	Alloy 617			ASME Draft Code Case for Alloy 617 (Maximum allowable temperature of 982°C)
Power Conversion System (PCS) Vessel	150°C	15X2NMFA (in Russia) 15Cr2NiMoVN		Kiryushin et al. 1997 EPRI 2002	ASME Section III, Subsection NB
Recuperator (including heat exchange surface)	Helium parameters for low/high pressure side: - Inlet 507.5°C, 2.63 MPa /108.1°C, 7.22 MPa - Outlet 127.3°C, 2.60 MPa /487.5°C, 7.15 MPa	Austenitic stainless steel 08Cr16Ni11Mo3		IAEA 2001	ASME Section III, Subsection NH (Maximum allowable temperatures of 816°C or lower – See Table 5)
Precooler and Intercooler	150°C (He) 60°C (air)	Type 321 SS		EPRI 2002	ASME Section III, Subsection NB

3 ASME Design Codes

3.1 Historical Background

Prior to World War II, the design of pressure vessels was based on selecting the thickness such that the maximum design pressure-induced stress in simple geometries was less than one-fifth the ultimate tensile strength (Cooper 1992). As a war emergency measure, this nominal factor of safety of five was reduced to four. Based on the success of this step, the codes were revised to adopt this lower factor of safety and questions arose as to the practicality of reducing the safety factor further. However, as the design technology including material behavior advanced, concerns were raised as to the need to include additional failure modes in the design of some vessels. These two aspects led to the development of Section III in 1963 and Section VIII Division 2 in 1968. The major conceptual change in these documents was in design, a change so significant that it was termed "Design by Analysis" to distinguish it from the approach previously followed, "Design by Rules." By and large the safety factors used in Design by Analysis were less conservative than those used in Design by Rules.

The basic intent of the code was to address the requirements for new constructions while providing reasonable assurance of reliable operation. Therefore, the requirements were primarily addressed to the manufacturer, although an important role was assigned to the owner/user with respect to defining the operational conditions to be considered by the manufacturer. The means by which the owner/user fulfilled this assigned responsibility was the preparation of a design specification.

A significant ground rule for the Design-by-Analysis procedures was to permit the application of elastic stress analysis techniques, even though practically all of the criteria were developed based on consideration of elastic-plastic failure modes (plastic collapse and necking, fatigue, ratcheting, etc.), because material selection requirements were intended to assure ductile behavior. Although it was intended that the gross behavior of the structure remain elastic, it was recognized that localized plastic deformation was not necessarily harmful. Therefore, a hopper diagram was developed to provide an orderly method of progressing through the design procedure in a manner which would assure the validity of the next step. For example, if stress amplitude satisfies the shakedown criterion ($3S_m$ criterion), then an elastic analysis was to provide stress amplitude that properly represented the plastic strain amplitude of interest in fatigue evaluations. Subsequently, alternative provisions permitted the use of elastic-plastic analyses with respect to most of the criteria, but up until the advent of advanced elastic-plastic finite-element analysis techniques, most of the design calculations in the early years were conducted with elastic stress analysis. Since most of the failure criteria addressed by the code are for plastic failure, the elastic analysis criteria are usually much more conservative than the elastic-plastic analysis criteria. The objective is to provide the designer with the option of satisfying less stringent rules at the expense of more detailed and rigorous analysis. Note that Section III has served as the model for almost all of nuclear design codes developed in other countries.

With the prospect of the construction of the liquid metal fast breeder reactor and high temperature gas-cooled reactor in the U.S. in the late 1960s and early 1970s, a need arose for the development of new Code rules applicable at "high temperatures," where ductile materials undergo thermal creep deformation that can lead to a new set of failure modes (creep rupture,

creep-fatigue, creep ratcheting, etc.) not experienced at the low temperatures for which the Section III rules were originally developed. The high-temperature design rules were initially developed as a series of code cases (e.g., Code Case 1331, Code Case 1592, and Code Case N47), which ultimately culminated in Subsection NH of Section III. Subsection NH (Code Case N47) has served as a template for several other code cases for elevated temperature service. Code Case N-499 was developed to address the use of SA-533 Grade B, Class 1 plate and SA-508 Class 3 forgings and their weldments for limited elevated temperature service. Code Case N-201 was developed for core support structures in elevated temperature service. A draft code case for Alloy 617 was in the process of being developed by the Task Group on Very-High Temperature Design before the activity was terminated. The draft Code Case employs a unified constitutive model that does not differentiate between plastic and creep deformation at high temperature (>650°C).

3.2 Basic ASME Code Definitions

Nuclear vessels and piping design criteria are governed by a combination of ASME Code and Nuclear Regulatory Commission (NRC) requirements. The main difference between low- and high-temperature requirements is not so much the effect of temperature, but the effect of time dependency that it introduces. In all other respects, the general design process is identical, and many of the notations used for low-temperature design are carried over to high-temperature applications. This section summarizes definitions of loading and stress categories used in the ASME Code design procedures, both in the low- and high-temperature sections. The design procedures including loading and stress classifications are common to Subsection NH, Code Case N-201, Code Case N-499, and draft code case for Alloy 617, although the allowable materials may vary.

3.2.1 Loading Categories

The following six loading categories are defined in the ASME Code (ASME 2001).

Design Loadings: The specified design parameters for the Design Loadings category equal or exceed those of the most severe combination of coincident pressure, temperature, and applied loads specified under events that cause Service Level A loadings described next.

Service Level A Loadings (Normal operation): These are loadings arising from system startup, operation in the design power range, hot standby, and system shutdown. Does not include service loadings covered by Levels B, C, and D or Test Loading.

Service Level B Loadings (upset conditions): These are deviations from Service Level A loadings that are anticipated to occur at moderate frequency. The events that cause Service Level B loadings include transients which result from any single operator error or control malfunction, transients caused by a fault in a system component requiring its isolation from the system, and transients due to loss of load or power. These events include any abnormal incidents not resulting in a forced outage.

Service Level C Loadings (emergency conditions): These are deviations from Service Level A loadings that have a low probability of occurrence and would require shutdown for correction of the loadings or repair of damage in the system. The total number of postulated occurrences for such events may not exceed 25.

Service Level D Loadings (faulted conditions): These are the combinations of loadings associated with extremely low probability, namely, postulated events whose consequences are such that the integrity and operability of the nuclear energy system may be impaired to the extent that only consideration of public health and safety are involved.

Test Loadings. These are pressure loadings that occur during hydrostatic tests, pneumatic tests, and leak tests. Other types of tests are classified as Service Level A or B loading. If any elevated temperature tests are specified as Test Loadings for a component, then these loadings shall be considered as part of Service Level B loadings.

Safety factors are highest for Level A, followed in decreasing order by Level B, C, and D.

3.2.2 Classification of Stresses

The basic premise behind classifying the stresses is that all stresses acting on a component made of ductile materials are not equal as far as the consequences of their presence are concerned. The stresses are characterized in the following three categories: primary stress, secondary stress, and peak stress.

Primary stress (P_m, P_L, and P_b) is any normal stress or a shear stress developed by an imposed loading which is necessary to satisfy the laws of equilibrium of external and internal forces and moments. The basic characteristic of a primary stress is that it is not self-limiting, cannot be relieved by localized plastic deformation, and if not limited, can lead to excessive plastic deformation of the structure. Primary stress is an algebraic sum of general or local primary membrane stress (P_m or P_L) and primary bending stress (P_b). Note that local primary membrane stress, P_L, includes the general primary membrane stress, P_m. The primary stresses are generally based on linear elastic theory.

Secondary stress (Q) is a normal or a shear stress developed by the constraint of adjacent material or by self-constraint of the structure. The basic characteristic of a secondary stress is that it is self-limiting, because it can be relieved by small-localized plastic deformation that cannot cause large distortion of the structure. Failure from one application of a secondary stress is not expected. Not all deformation-controlled stress can be categorized as secondary stress. The code requires all deformation-controlled stress with high elastic followup to be treated as primary stress. Often, membrane components of thermal stresses are categorized as primary.

Peak stress (F) is due to local discontinuities or local thermal stress including the effects of stress concentration. This stress is additive to the primary plus secondary stress. The basic characteristic of a peak stress is that it does not cause any noticeable distortion. The peak stress is objectionable only as a possible source of a fatigue crack or a brittle failure.

To handle components under a multiaxial stress state, the code requires the use of effective stress or stress intensity based on the maximum shear stress (Tresca) criterion.

3.3 ASME B&PV Code, Section III, Subsection NB

In the ASME Code, structural integrity of a component below the creep range is assured by providing design margins against the following failure modes:

1. Failure by plastic instability or necking,
2. General structural collapse under a single application of limit load,
3. Time-independent buckling,
4. Incremental collapse or ratcheting under cyclic loading,
5. Fatigue under cyclic loading, and
6. Fast fracture.

The first two failure modes challenge the ability of the component to resist permanent distortion and/or plastic instability under a single application of the maximum anticipated load; the third failure mode is buckling of a slender component due to compressive loading; the next two failure modes challenge the ability of the component to survive a succession of the same and/or different loads; and the final failure mode challenges the defect tolerance of the component. Rules are given in the code to protect against these failure modes using either elastic or plastic analysis techniques.

3.3.1 Limits for Primary Stress

Elastic Analysis Rules

The fundamental allowable stress in the ASME Code is the S_m, which is defined as follows:

$$S_m = \min\left\{\frac{1}{3} S_u, \frac{2}{3} S_y\right\} \tag{1}$$

where S_u and S_y are the ultimate tensile and yield strengths, respectively, at a given temperature.[1] The factor 3 on S_u is a safety factor against rupture by plastic instability or necking, and the factor 1.5 on S_y is a safety factor against failure by plastic collapse. Virtually all the nuclear design codes [RCC-MR (France), R5 (UK), MITI Notification No. 501 (Japan), PNEAG–7–002–86 (RF), etc.] use the same or a similar definition for a general primary membrane stress limit. To apply the rules, data are needed on yield (S_y) and ultimate tensile strengths (S_u) as functions of temperature.

[1]The factor 2/3 is replaced by 0.9 for highly strain-hardening material like austenitic stainless steels.

Limits for General Primary Membrane Stress

The ASME Code requires that for normal operation and upset conditions (Service Level A and B loadings)

$$P_m \leq S_m \tag{2a}$$

For upset conditions (Level B loading), the value of S_m above may be increased by 10%. For emergency conditions (Service Level C loading), the allowable general primary membrane stress intensity is

$$P_m \leq \max \begin{cases} 1.2 S_m \\ S_y \end{cases} \tag{2b}$$

In addition, for ferritic materials, the following limit applies

$$P_m \leq \max \begin{cases} 1.1 S_m \\ 0.9 S_y \end{cases} \tag{2c}$$

For faulted conditions (Service Level D loading), the allowable general primary membrane stress intensity is

$$P_m \leq \begin{cases} 2.4 S_m \\ 0.7 S_u \end{cases} \tag{2d}$$

Equations (1) and 2(a-c) ensure that the primary stress, which is in static equilibrium with external loads, stays below either the yield or the ultimate strength during normal operation, upset, and emergency conditions. This mitigates failure modes 1 and 2. On the other hand, Equations (1) and (2d) ensure that the primary stress during faulted condition stays below the ultimate tensile strength (preventing rupture, i.e., failure mode 1) but may exceed the yield stress, which in turn, may lead to significant plastic deformation.

Limits for Local Primary Membrane and Primary Bending Stress

The ASME Code requires that for normal operation and upset conditions (Service Levels A and B loadings)

$$P_L + P_b \leq K S_m \tag{3a}$$

where K (≤ 1.5) represents the ratio between the loads to cause fully plastic section and initial yielding in the extreme fiber of the section. For shells and solid sections, K = 1.5. For upset conditions (Level B loadings), the value of S_m may be increased by 10%.

For emergency conditions (Service Level C loading), the allowable local primary membrane-plus-bending stress intensity is

$$P_L + P_b \leq \begin{cases} 1.2 K S_m \\ K S_y \end{cases} \tag{3b}$$

For faulted conditions (Service Level D loading), the allowable local primary membrane-plus-bending stress intensity is

$$P_L + P_b < \begin{cases} 3.6S_m \\ 1.05S_u \end{cases} \quad (3c)$$

Equations (1), (3a), and (3b) ensure that the primary membrane plus bending stress, which is in static equilibrium with external loads, does not exceed the collapse load during normal operation, upset, and emergency conditions. According to the Lower Bound Theorem of plasticity, the external loads represent a lower bound on the true collapse load. Thus, these equations ensure that failure mode 2 cannot occur. However, significant plastic deformation may occur under faulted conditions.

Plastic Analysis Rules

Either plastic collapse load analysis (with a perfectly-plastic stress-strain curve) or detailed plastic analysis (e.g., finite element analysis), with or without geometric nonlinearity, conducted with the actual stress-strain curve (including strain hardening) can be used to satisfy the primary stress limits. Thus, to apply plastic analysis, stress-strain curves at various temperatures are needed.

Collapse Load Analysis

The elastic analysis rules for general primary membrane stress, local primary membrane stress, and primary bending stress need not be satisfied if plastic limit analysis techniques are used to show that the specified loads do not exceed two-thirds the lower bound collapse load. The yield strength to be used in these calculations is $1.5S_m$.

For faulted conditions (Level D loading), the elastic analysis rules for general primary membrane stress, local primary membrane stress, and primary bending stress need not be satisfied if plastic limit analysis techniques are used to show that the specified loads do not exceed 90% of the limit analysis collapse load. The yield strength to be used in these calculations is the lesser of $2.3S_m$ and $0.7S_u$.

Plastic Analysis

The elastic analysis rules for general primary membrane stress, local primary membrane stress, and primary bending stress need not be satisfied if detailed plastic analysis is used to show that the specified loads do not exceed two-thirds the lower bound collapse load as determined from the load-deflection or load-strain relationship obtained by plastic analysis.

For faulted conditions (Level D loading), the elastic analysis rules for general primary membrane stress, local primary membrane stress, and primary bending stress need not be satisfied if plastic analysis is used, in which case the following conditions apply:

$P_m \le \max \begin{cases} 0.7S_u \\ S_y + 1/3\left(S_u - S_y\right) \end{cases}$ for austenitic steels and high nickel alloys, and

$P_m \le 0.7S_u$ for ferritic steels

$P_L + P_b \leq 0.9S_u$

Average primary shear stress across a section loaded in pure shear $\leq 0.42\ S_u$

3.3.2 Low-Temperature Limits for Cyclic Loading

All the design codes assume that the material has sufficient ductility so that failure by a single application of the primary plus secondary stresses does not lead to rupture. However, all codes recognize that repeated application of secondary stresses in the presence of a steady primary stress may lead to failure by cyclic plastic ratcheting (failure mode 4), and repeated application of cyclic primary and secondary stresses (membrane plus bending plus peak) may lead to failure by fatigue (failure mode 5). To prevent such failures, the code provides limits using either elastic analysis or plastic analysis. Elastic analysis rules are discussed in this section. The plastic analysis rules are given in Section 3.3.3.

Elastic Analysis Rules

To ensure that results from elastic analysis are applicable to the elastic ratcheting and elastic fatigue rules, the code limits the maximum value of the cyclic primary-plus-secondary stress range.

Limits for Primary-Plus-Secondary Stress

For normal operation (Service Level A loading),

$$\Delta(P_L + P_b + Q) \leq 3S_m \tag{4a}$$

The rationale behind this rule is that as long as the range of the primary-plus-secondary stresses is within the yield envelope (note $3S_m \leq 2S_y$) at every point in the component, it will eventually reach a fully elastic state by building up a residual stress field. This rationale reflects the concept of shakedown, which ensures that ratcheting does not occur, although a small amount of plastic strain may accumulate prior to shakedown. Equation (4a) is also a pre-requisite for satisfying fatigue life requirements with elastic analysis results. For upset conditions (Service Level B loading),

$$\Delta(P_L + P_b + Q) \leq 3.3S_m \tag{4b}$$

For emergency conditions (Service Level C loading),

$$\Delta(P_L + P_b + Q) \leq 3.6S_m \tag{4c}$$

3.3.3 Low-Temperature Ratcheting Limits

Elastic Analysis Rule

The ASME Code also contains an explicit thermal ratcheting rule based on a Bree diagram (Figure 3.1) that is applicable to axisymmetric shell structures subjected to internal pressure and thermal stresses caused by a linear through-thickness temperature gradient.

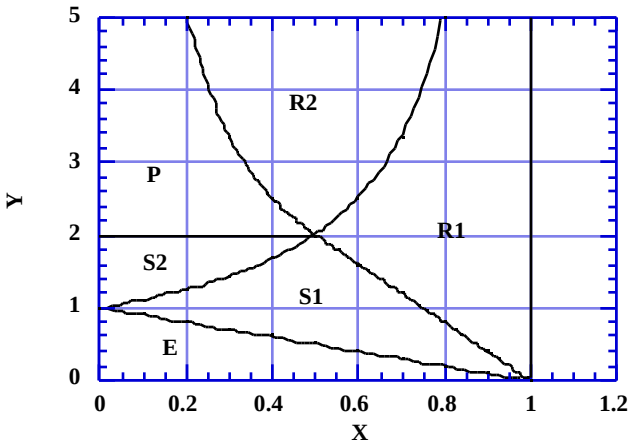

Figure 3.1. Bree diagram for axisymmetric shell under steady internal pressure and cyclic thermal stress due to linear through-thickness temperature gradient.

In Figure 3.1,

$$X = \frac{P_L}{S_y} \text{ and } Y = \frac{\Delta Q}{S_y}, \tag{5a}$$

where S_y is the yield stress, and the steady primary (P_L) and cyclic secondary stress intensities (ΔQ) are calculated by elastic stress analysis. The regimes R1 and R2 represent loading combinations that lead to cyclic ratcheting and are not permitted in the ASME code. Regimes S1 and S2 lead to shakedown; P leads to cyclic plasticity and E is the elastic regime. Note that for non-axisymmetric structures, the Bree diagram shown in Figure 3.1 is not necessarily applicable. The Bree diagram limits can be expressed as follows:

$$Y = \begin{cases} \dfrac{1}{X} & \text{for } 0 < X < 0.5 \\ 4(1 - X) & \text{for } 0.5 < X < 1 \end{cases} \tag{5b}$$

The ratcheting rule is applicable to Level A and B loadings only. Level C and D loadings are exempt from the ratcheting rule because they involve a limited number of cycles.

Plastic Analysis Rule

The limit on thermal stress ratchet can be demonstrated by conducting plastic analysis to show that shakedown occurs (as opposed to continuous deformation). However, this shakedown requirement need not be satisfied for materials with $S_{y,min}/S_{u,min} \leq 0.7$, provided the maximum accumulated plastic strain at any point is ≤ 5%.

3.3.4 Low-Temperature Fatigue Limit

Elastic Analysis Rule

Peak stresses due to stress concentration effects are only relevant when dealing with potential failure mechanisms (e.g., fatigue) that depend on the local state of stress. The ASME code requires that the total stress range due to Service Level A and B loadings must satisfy,

$$\Delta(P_L + P_b + Q + F) \leq 2S_a \tag{6}$$

where S_a, the stress amplitude corresponding to the required number of design cycles, N_d, is obtained from Appendix I. Thus, Equation 6 addresses failure mode 5. Service Level C and D loadings are exempted from fatigue analysis because of the limited number of cycles. If there are two or more types of stress cycles, a linear cycle-fraction cumulative damage rule is applied by using the concept of usage factors (U_i). The cumulative usage factor U for n types of stress cycles is defined as

$$U = \sum_{i=1}^{n} U_i = \sum_{i=1}^{n} \frac{n_i}{N_{di}} \tag{7a}$$

where U_i is the usage factor for the n_i number of cycles of the ith type at stress amplitude S_{ai}, and N_{di} is the allowable fatigue cycles corresponding to S_{ai}. The total cumulative usage factor is limited to one:

$$U \leq 1 \tag{7b}$$

The linear cycle-fraction cumulative damage rule ignores sequence effects even though data show that the sequence of high-low stress cycles often leads to a lower number of cycles to failure than the reverse low-high cycles. To apply the fatigue design rule, mean fatigue curves obtained by laboratory tests at various temperatures and relevant environments are needed. The design fatigue curves in Appendix I are derived from the mean fatigue curves in air after applying a factor of two on stress and twenty on life, whichever is more conservative (Langer 1962, Jaske and O'Donnell 1977).

Plastic Analysis Rule

The $3S_m$ limit on the range of primary-plus-secondary stress intensity range may be exceeded, provided the following simplified elastic-plastic analysis rules are used

(1) The primary-plus-secondary membrane stress intensity range plus bending stress intensity range (using elastic analysis), excluding thermal bending stresses, satisfies the $3S_m$ limit.

(2) The elastic thermal ratcheting rule is satisfied.

(3) The value of S_a to enter the design fatigue curve is multiplied by K_e, where

$K_e = 1$ for $S_n \leq 3S_m$

$K_e = 1.0 + [(1-n)/n(m-1)](S_n/3S_m - 1)$ for $3S_m \leq S_n < 3mS_m$

$K_e = 1/n$ for $3mS_m \leq S_n$

where S_n is the primary-plus-secondary stress intensity range. Values of material parameters m and n are given in Section III for carbon steels, low alloy steels, martensitic stainless steels, austenitic stainless steels, nickel-chromium-iron alloys, and nickel-copper alloys. Values of m and n have to be determined for materials not listed.

(4) The rest of the fatigue evaluation stays the same as for the elastic fatigue rules.

3.3.5 Low-Temperature Fast Fracture

Section III of the code does not contain any explicit requirements for preventing fast (nonductile) fracture because the accepted materials are generally ductile and have high toughness. However, nonmandatory guidance for preventing nonductile fracture in ferritic steel (which undergoes ductile-brittle transition) at pressure-retaining boundaries is given in Appendix G for Service Level A and B loadings. This guidance is based on linear elastic fracture mechanics. For section thickness between 10 cm (4 in.) and 30 cm (12 in.) a defect of depth one-fourth the section thickness and length 1.5 times the section thickness is postulated. For section thickness greater than 30 cm, the postulated defect for 30-cm thickness is recommended. For sections less than 10 cm (4 in.) thick, a 2.5-cm (1-in.) deep defect is conservatively postulated. In the absence of data, a reference critical stress intensity factor K_{IR} is provided:

$$K_{IR} = 26.78 + 1.223 \exp[0.0145(T - RT_{NDT} + 160)] \quad (8)$$

where K_{IR} is in ksi$\sqrt{\text{in}}$, temperature T is in °F, and RT_{NDT} is the reference nil ductility temperature in °F. To be conservative, a factor of 2 is applied on the stress intensity factor for primary stresses, and the following limits are required to be satisfied:

$$2K_{Im} + K_{It} < K_{IR} \quad (9a)$$

where K_{Im} is the stress intensity factor due to primary membrane stress, and K_{It} is the stress intensity factor due to secondary (thermal) membrane stress, and

$$2K_{Im} + 2K_{Ib} + K_{It} + K_{Itb} < K_{IR} \quad (9b)$$

where K_{Ib} is the stress intensity factor due to primary bending stress, and K_{Itb} is the stress intensity factor due to secondary (thermal) bending stress.

3.3.6 Buckling Limits

The design limits of Subsection NB guard against time-independent (instantaneous) buckling. These limits are applicable only to certain geometrical configurations under specific loading conditions, in particular, cylindrical shells under external pressure or axial compression, with or without stiffeners, and spherical shells under external pressure. These limits include the effects of initial geometrical imperfections permitted by fabrication tolerances on vessel shells. However, these limits do not consider effects of creep due to long-term loading at elevated temperatures and the effects of other loads or other geometries.

3.4 ASME B&PV Code, Section III, Subsection NH

Subsection NH of ASME B&PV Code, Section III, provides high-temperature design rules for construction of Class 1 components having metal temperatures exceeding those covered by the rules and stress limits of Subsection NB and Tables 2A, 2B, and 4 of Section II, Part D, Subpart 1. Table 3.1 lists the materials included in Subsection NH along with the maximum temperatures permitted.

Table 3.1. Maximum allowable temperatures for the materials included in Subsection NH

Material	Maximum Allowable Metal Temperature, °C[1]
304 SS	816
316 SS	816
Alloy 800H	760
2.25 Cr-1 Mo	593[2]
Alloy 718	566

[1]Maximum allowable time at this temperature is 300,000 hours.
[2]Higher temperature (649°C) is allowed for the maximum allowable time of 1,000 hours at this temperature.

3.4.1 High-Temperature Design Rules

The first step in design for elevated temperature is to design the component for low-temperature operation. The first few steps in the design process are, therefore, identical with those used in low-temperature applications. Operation at elevated temperature introduces time-dependent failure modes. Thus, in addition to the six time-independent failure modes addressed in Section 3.3, the following six time-dependent failure modes are considered in the high-temperature design:

1) Creep rupture under sustained primary loading,

2) Excessive creep deformation under sustained primary loading,

3) Cyclic creep ratcheting due to steady primary and cyclic secondary loading,

4) Creep-fatigue due to cyclic primary, secondary, and peak stresses,

5) Creep crack growth and nonductile fracture, and

6) Creep buckling.

Rules are given in Subsection NH to protect against these failure modes using elastic and, in some cases, either elastic or elastic-plastic analysis techniques.

3.4.2 Material Properties Database Needed

To carry out high-temperature design, the following mechanical properties as functions of temperature are needed, from which the design allowables are derived after applying appropriate safety factors:

1) Modulus of elasticity and Poisson's ratio (average),

2) Yield strength (average and minimum),

3) Ultimate tensile strength (average and minimum),

4) Stress-strain curves (average and minimum),

5) Stress vs. creep rupture time for base metals and their weldments (average and minimum),

6) Stress vs. time to 1% total strain (average),

7) Stress vs. time to onset of tertiary creep (minimum),

8) Constitutive equations for conducting time- and temperature-dependent stress-strain analysis (average),

9) Isochronous stress-strain curves (average),[1]

10) Continuously cycling fatigue life as a function of strain range at a fast strain rate (average), and

11) Creep-fatigue cyclic life involving cycles with various strain ranges and hold times (average).

Any loss or change in mechanical properties caused by thermal aging, decarburization, etc., with long-term high-temperature exposure in an environment should also be included in the database. Items 4 and 8 are needed for conducting inelastic stress-strain analyses. The rest are required for satisfying elastic as well as inelastic analysis limits.

3.4.3 Primary Stress Limits

Elastic Analysis Rules

Time-Dependent Primary Stress Limit for Base Metal

In addition to the time-independent S_m, the code introduces a temperature- and time-dependent quantity S_t to account for creep effects. For each specific time t and temperature T, S_t for the base metal is defined as the lesser of the following three stresses:

(1) 100% of the average stress required to obtain a total (elastic, plastic, primary creep, and secondary creep) strain of 1%;

(2) 80% of the minimum stress to cause initiation of tertiary creep; and

(3) 67% of the minimum stress to cause rupture.

[1]Isochronous curves are constructed by cross-plotting conventional constant stress strain/time curves on stress/strain axes, to form a series of isochronous contours, representing the strain produced at a prescribed stress, in a certain time.

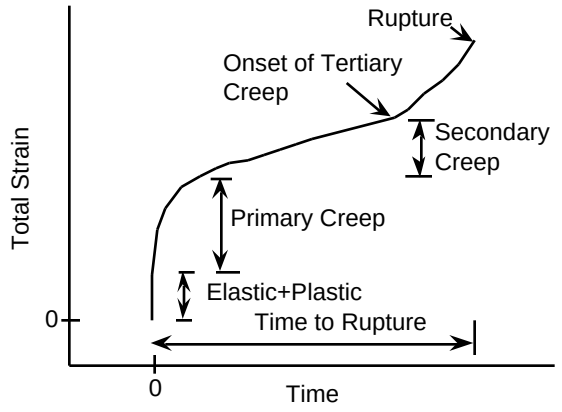

Figure 3.2a. Classical creep curve

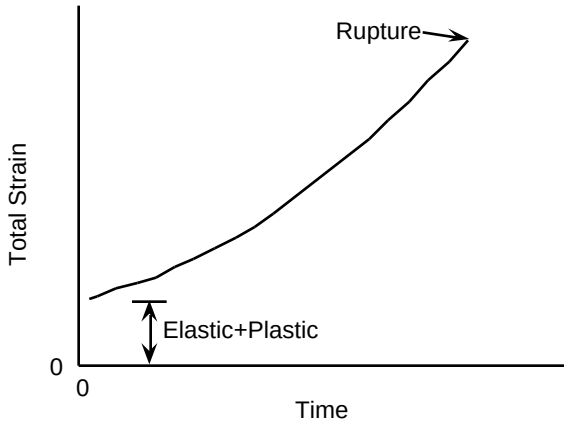

Figure 3.2b. Nonclassical creep curve

A basic primary stress limit for high temperatures is S_{mt}, which is the lesser of S_m and S_t, and is a function of both time and temperature. Note that the definition of S_t assumes that the material has a classical creep curve (Figure 3.2a). However, some nickel alloys exhibit a nonclassical creep curve (Figure 3.2b) with no clear primary creep or secondary creep regime. The above definition of S_t has to be revised for these materials.

Time-dependent Primary Stress Limit for Weldments

The basic primary stress limit for weldment at high temperatures is the lesser of S_{mt} of the base metal and $0.8S_rR$, where S_r is the expected minimum stress-to-rupture strength of the base metal, and R is the appropriate ratio between the creep rupture strength for the weld metal and the base metal. The time- and temperature-dependent stress intensity limit S_t for weldment is the lesser of S_t for the base metal and $0.8S_rR$.

Limits for General Primary Membrane Stress

The ASME Code requires that for normal operation and upset conditions (Service Level A and B loadings)

$$P_m \le S_{mt} \tag{10a}$$

For emergency conditions (Service Level C loading), the allowable general primary membrane stress intensity is

$$P_m \le \begin{cases} 1.2\,S_m \\ S_t \end{cases} \tag{10b}$$

In addition, the time-based use-fraction sum associated with the general primary membrane stresses for Level A, B, and C primary loadings shall be less than 1.

For faulted conditions (Service Level D loading), the limits on allowable general primary membrane stress intensity, obtained in part from Appendix F of Section III, is

$$P_m < \begin{cases} 2.4 S_m \\ 0.7 S_u \\ 0.67 S_r \\ 0.8 R S_r \end{cases} \quad (10c)$$

In addition, the time-based use-fraction sum associated with the general primary membrane stresses for all service loadings shall be less than 1.

Equations [10(a-b)] ensure that the primary stress, which is in static equilibrium with external loads, stays below the yield and the ultimate strength, and keeps the maximum thickness-averaged creep strain to ≤1% during normal operation, upset, and emergency conditions. This condition mitigates failure modes 1, 2, 7, and 8. On the other hand, Equation 10c ensures that the primary stress during faulted condition stays below the ultimate tensile and creep rupture strengths (preventing rupture, i.e., failure modes 1 and 7) but may exceed the yield stress, which in turn, may lead to significant plastic deformation.

Limits for Local Primary Membrane and Primary Bending Stress

The ASME Code requires that for normal operation and upset conditions (Service Level A and B loadings)

$$P_L + P_b \le K S_m \quad (11a)$$

$$P_L + P_b / K_t \le S_t \quad (11b)$$

where K_t accounts for relaxation of extreme fiber bending stress due to creep. The factor is given by

$$K_t = (K + 1)/2 \quad (11c)$$

where K (≤ 1.5) represents the ratio between the loads to cause fully plastic section and initial yielding in the extreme fiber of the section. For shells and solid sections, K = 1.5.

For emergency conditions (Service Level C loading), the allowable local stress intensity for the primary membrane-plus-bending is

$$P_L + P_b \le 1.2 K S_m \quad (11d)$$

$$P_L + P_b / K_t \le S_t \quad (11e)$$

In addition, the time-based use-fraction sum associated with the local primary membrane-plus-bending stresses for Level A, B, and C primary loadings shall be less than 1.

For faulted conditions (Service Level D loading), the allowable local primary membrane-plus-bending stress intensity is

$$P_L + P_b < \begin{cases} 3.6 S_m \\ 1.05 S_u \end{cases} \quad (11f)$$

$$P_L + P_b / K_t \le \begin{cases} 0.67 S_r \\ 0.8 R S_r \end{cases} \qquad (11g)$$

In addition, the time-based use-fraction sum associated with the local primary membrane-plus-bending stress intensity for all service loadings shall be less than 1.

Equations [11(a-b)] and [11(d-e)] ensure that the primary membrane-plus-bending stress, which is in static equilibrium with external loads, does not exceed the collapse load or cause excessive creep deformation during normal operation, upset, and emergency conditions. According to the Lower Bound Theorem of plasticity, the external loads represent a lower bound on the true collapse load. Thus, these equations ensure that failure modes 2 and 8 cannot occur. However, significant plastic deformation but no rupture may occur under faulted conditions.

Creep Bending Shape Factor K_t

Assuming a simple Norton's power law creep, we can show that Equation (11c) for K_t is conservative for solid rectangular sections as long as the creep exponent is >3 (Figure 3.3).

Inelastic Analysis Rules

Subsection NH does not include inelastic analysis rules for satisfying the primary stress limits. However, the inelastic strain limits in Section 3.4.5 have to be satisfied.

3.4.4 High-Temperature Limits for Cyclic Loading

When creep effects are significant [T >427°C (800°F) for austenitic stainless steels and >371°C (700°F) for ferritic steels], inelastic analysis is generally required to quantitatively assess strains and deformations. However, elastic and simplified inelastic analysis methods

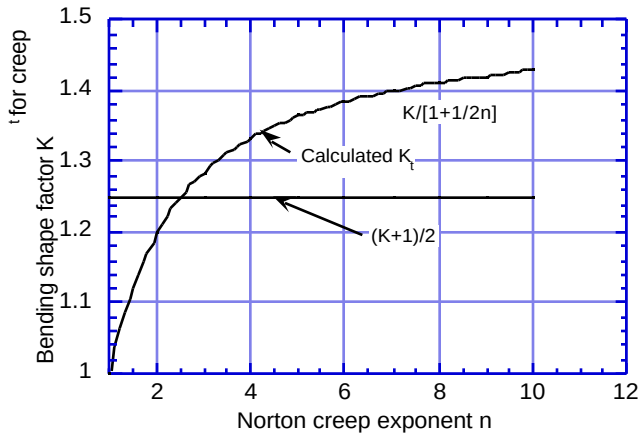

Figure 3.3. Variation of high-temperature effective bending shape factor K_t for creep with Norton creep exponent.

can sometimes be justified and used to establish conservative bounds for deformation, strain, strain ranges, and maximum stress in order to reduce the number of locations needed for detailed inelastic analysis. Note that the multiaxial constitutive equations needed to perform detailed inelastic analyses might not be available for some materials. Nonmandatory rules for strain, deformation, and fatigue limits at elevated temperature are contained in non-mandatory Appendix T of Subsection NH. These rules can be satisfied either by elastic or inelastic analysis.

3.4.5 High-Temperature Ratcheting Limits

The objective of the ratcheting rules is to ensure that the maximum accumulated principal tensile inelastic stain at any point over the expected operating lifetime of the equipment due to Level A, B, and C loadings does not exceed the inelastic strain limits. Strain limits need not be satisfied for Level D loading.

Inelastic Strain Limits for Base Metal

The inelastic strain limits for base metal are as follows:

1) strains, average through thickness, 1%;

2) strains at the surface, due to an equivalent linear distribution through the thickness, 2%;

3) local strains at any point, 5%.

Inelastic Strain Limits for Welds

Because of the potential for limited ductility of weld metal at elevated temperatures and the potential for high strain concentrations (both metallurgical and geometric) in the heat-affected zones of weldments, inelastic strains accumulated in the weld region (defined as ±3 times the thickness to either side of the weld centerline) shall not exceed one-half of that permitted for the parent material.

Elastic Analysis Rules

The inelastic strain limits are considered to have been satisfied if any of the Tests A1, A2 or A3 (in decreasing order of conservativeness) is satisfied. The tests are expressed in terms of X and Y, which are defined in terms of the maximum local primary membrane-and-bending stress intensities and maximum range of secondary stress intensity, and the average yield stress during the cycle, as follows:

$$X = \frac{\left(P_L + P_b / K_t\right)_{max}}{S_{y,avg}} \tag{12a}$$

and

$$Y = \frac{\left(\Delta Q\right)_{max}}{S_{y,avg}} \tag{12b}$$

For Test A1,

$$X + Y \leq S_a / S_y \tag{13}$$

where S_a is the lesser of

(a) $1.25S_t$ using the highest wall-averaged temperature during the cycle and a time of 10^4 h, and

(b) the average of two S_y values associated with the maximum and minimum wall-averaged temperatures during the cycle.

For Test A2,

$$X + Y \leq 1 \tag{14}$$

for those cycles during which the average wall temperature at one of the stress extremes defining the maximum cyclic primary-plus-secondary stress range is below the temperature where creep is negligible.

Test A3 can can be applied if the following conditions are first met:

(a) the low-temperature $3S_m$ rule (Eq. 4a) is satisfied,

(b) the low-temperature Bree diagram rule (Eq. 5) is satisfied,

(c) $W_t\left[1.5S_y(T_m)\right] \leq 0.1$

where W_t is the creep rupture usage fraction evaluated using a stress 1.5 times the average yield strength at maximum wall-averaged temperature T_m during each interval

(d) $\sum_i \varepsilon_i\left[1.25S_y(T_{m,i})\right] \leq 0.2\%$

where ε_i is the creep strain at a stress of 1.25 times the average yield strength at maximum wall-averaged temperature $T_{m,i}$ during interval i.

If conditions (a) through (d) are met, then

$$\Delta\left(P_L + P_b\right)_{max} + \Delta\left[Q\right]_{max} \leq 3\,\overline{S_m} \tag{15}$$

where $3\,\overline{S_m}$ is the lesser of $3S_m$ and

$1.5S_m + 1.5\,S_{rH}$ if only one extreme of the stress cycle occurs at a temperature above which creep is not negligible, and

$S_{rH} + S_{rL}$ if both extremes of the stress cycle occur at temperatures above which creep is not negligible,

Where S_{rH} and S_{rL} are the relaxation strengths associated with the "hot" and "cold" extremes of the stress cycle.

Simplified Inelastic Analysis Rules

The simplified inelastic strain analysis has three tests.

Test No. B1

The inelastic strain limits are considered to be satisfied if the following conditions are met first:

(a) The structure must be either axisymmetric with axisymmetric loading away from local structural discontinuity or a general structure in which the peak through wall thermal stress is negligible, i.e., the thermal through-wall stress distribution is approximately linear.

(b) The individual cycles defined in the design specification cannot be split into subcycles.

(c) Secondary stresses with elastic followup (i.e., pressure-induced membrane and bending stresses and thermal-induced membrane stresses) should be classified as primary stresses.

(d) At least one extreme of the stress cycle occurs at a temperature below which creep is negligible.

(e) Load combinations in the R_1 and R_2 ratcheting regimes in Figure 3.4 are not permitted.

If conditions (a) through (e) are satisfied, then

- Divide the service life into N time-temperature blocks.
- Determine the effective creep stress $\sigma_{c,k}$.for the kth (k = 1 to N) time-temperature block using the formula

$$\sigma_c = Z\, S_{yL} \tag{16a}$$

where S_{yL} is the S_y value at the "low" temperature extreme of the cycle, and Z is a creep stress parameter for any combination of loading given in Figure 3.4. Z may be calculated as follows.

In regimes S_2 and P,

$$Z = X \cdot Y \tag{17a}$$

In regime S_1,

$$Z = Y + 1 - 2\sqrt{(1-X)Y} \tag{17b}$$

In regime E,

$$Z = X \tag{17c}$$

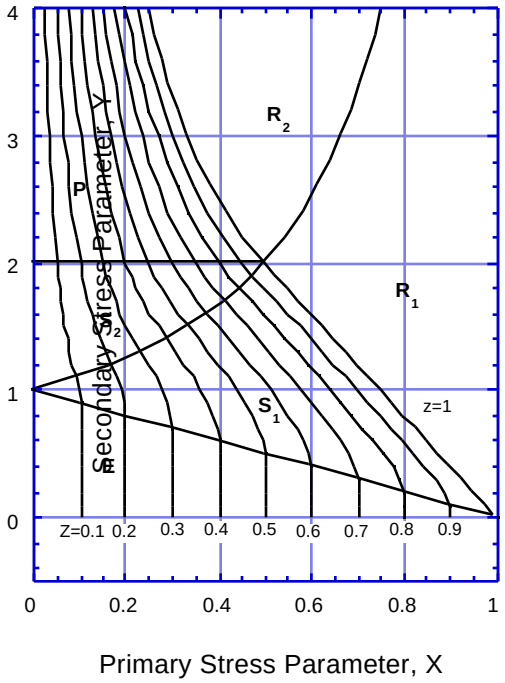

Figure 3.4. Effective creep stress parameter Z for simplified inelastic analysis rules B1 and B3.

where the definitions of X and Y are the same as given in Equations (12a-b), except that the S_y value is replaced by S_{yL}.

Test No. B-1 is applicable only if σ_c values calculated above for all the blocks are less than their corresponding hot yield stress S_{yH} which is the S_y value at the "high" temperature extreme of the cycle. If so,

- Multiply each value of $\sigma_{c,k}$ by 1.25, and evaluate the creep strain increment associated with the stress $1.25\sigma_{c,k}$ held constant throughout the particular time-temperature block, using the isochronous sress-strain curves.

- Limit the maximum value of the accumulated creep strain to 1% for the base metal.

- Limit the maximum value of the accumulated creep strain to 0.5% for the weld metal.

The code also gives a more conservative ratcheting rule for any general structure which is similar to Test B1, with the exception that the effective creep stress parameter Z is obtained from a figure in the code. This is Test B2.

Test B3 is the least conservative of the three tests and is the only test that permits load combinations, which lie in the ratcheting regimes R1 and R2 in Figure 3.4. However, it is restricted to axisymmetric structures with axisymmetric loading away from local structural discontinuity. The code gives explicit equations for calculating bounds to ratcheting plastic

strains and enhanced creep strains due to creep relaxation within the cycles in the S_1, S_2, P, R_1, and R_2 regimes in Figure 3.4. These strains have to be added to the accumulated inelastic strain calculated by Test B1 using isochronous stress-strain curves.

3.4.6 High-Temperature Creep-Fatigue Rule

Damage Equation

The combination of Level A, B, and C loadings shall be evaluated for accumulated creep and fatigue damage, including hold time and strain rate effects. For a design to be acceptable, the creep and fatigue damage shall satisfy the following relation:

$$\sum_{j=1}^{p} \left(\frac{n}{N_d}\right)_j + \sum_{k=1}^{q} \left(\frac{\Delta t}{T_d}\right)_k \le D \tag{18}$$

where D = the total creep-fatigue damage (Figure 3.5); $(N_d)_j$ = number of design allowable fatigue cycles for cycle type j at a given total equivalent strain range, temperature, and high strain rate ($\geq 10^{-3}/s$); $(T_d)_k$ = allowable duration (obtained from the minimum time-to-rupture plot) for a given stress and maximum temperature at the point of interest and occurring during the time interval k; $(n)_j$ = number of repeated cycles of type j; and $(\Delta t)_k$ = duration of time interval k.

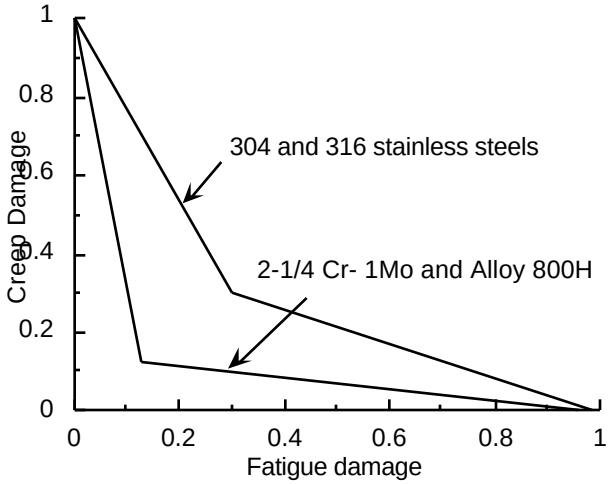

Figure 3.5. Creep-fatigue damage envelope for both elastic and inelastic analysis rules.

The equivalent strain range is defined with respect to changes in the strain components from the starting point to each point j in the cycle,

$$\Delta\varepsilon_{eq,j} = \frac{\sqrt{2}}{2(1+\nu^*)}\left[\left(\Delta\varepsilon_{x,j} - \Delta\varepsilon_{y,j}\right)^2 + \left(\Delta\varepsilon_{y,j} - \Delta\varepsilon_{z,j}\right)^2 + \left(\Delta\varepsilon_{z,j} - \Delta\varepsilon_{x,j}\right)^2 + \frac{3}{2}\left(\gamma_{xy,j}^2 + \gamma_{yz,j}^2 + \gamma_{zx,j}^2\right)\right]^{1/2} \tag{19}$$

where

$$\nu^* = \begin{cases} 0.3 \text{ for elastic analysis rule} \\ 0.5 \text{ for inelastic analysis rule} \end{cases}$$

$$\Delta\varepsilon_{max} = Max[\Delta\varepsilon_{eq,j}) \quad (20)$$

Satisfaction of Creep-Fatigue Limits Using Elastic Analysis

The elastic analysis rule can be used only if

(1) elastic ratcheting rule A1, A2 or A3 is satisfied or simplified inelastic analysis ratcheting rule B1 is satisfied with $Z \leq 1$,

(2) the $3S_m$ rule [Equation (4a)] is satisfied with $3S_m$ being defined as the lesser of $3S_m$ and $3\overline{S_m}$ as defined in Equation (15), and

(3) thermal induced membrane stress is classified as primary stress.

Fatigue Damage Evaluation

If the above conditions are satisfied, then the elastic analysis rule can be applied by first modifying the equivalent strain range for each cycle type from $\Delta\varepsilon_{max}$ to $\Delta\varepsilon_{mod}$ to account for stress concentration factor K using Neuber's rule. Three options with different degrees of conservatism are provided in the code. The total strain range (ε_t) that is entered in the fatigue design curve to obtain N_d [Equation (18)] is finally calculated as follows:

$$\varepsilon_t = K_\nu \Delta\varepsilon_{mod} + K \Delta\varepsilon_c \quad (21)$$

where

K = local geometrical stress concentration factor

K_ν = the multiaxial plasticity and Poisson's ratio adjustment factor

$\Delta\varepsilon_c$ = creep strain increment during each cycle

Formulas for calculating K_ν and $\Delta\varepsilon_c$ are given in the code.

Creep Damage Evaluation

Appendix T gives two options for evaluating the creep damage during hold periods by providing upper-bound estimates of creep strain accumulation and variation of stress due to stress relaxation, using the isochronous stress-strain curves. As an added conservatism, the stress during an incremental time during the hold period is divided by factor K' (=0.67) before it is entered in the minimum time-to-rupture plot to obtain T_d in Equation (18).

Satisfaction of Creep-Fatigue Limits Using Inelastic Analysis

With the inelastic analysis, the calculated equivalent strain range already incorporates stress concentration effects, and no further adjustment is necessary. It can be entered in the fatigue design curve to obtain N_d. The creep damage in Equation (18) may be replaced by an integral

$$\int_{t=0}^{t} \frac{dt}{T_d}$$

where T_d is obtained from the minimum time-to-rupture curve. The effective stress σ_e for the multiaxial stress state is defined as follows:

$$\sigma_e = \bar{\sigma} \exp\left[C\left(\frac{J_1}{S_S} - 1\right)\right] \tag{22}$$

where

$$\bar{\sigma} = \frac{1}{\sqrt{2}}\left[(\sigma_1 - \sigma_2)^2 + (\sigma_2 - \sigma_3)^2 + (\sigma_3 - \sigma_1)^2\right]^{1/2} \tag{23a}$$

$$J_1 = \sigma_1 + \sigma_2 + \sigma_3 \tag{23b}$$

$$S_S = \left[\sigma_1^2 + \sigma_2^2 + \sigma_3^2\right]^{1/2} \tag{23c}$$

where σ_1, σ_2, and σ_3 are the principal stresses. As in the elastic analysis case, the effective stress σ_e is divided by K' (=0.67) before the minimum time-to-rupture curve is entered to obtain T_d. The constant C is equal to 0.24 for austenitic stainless steels and 0 for 2-1/4Cr-1Mo and Alloy 800H.

Creep Fatigue of Weldment

Because of the potential for limited ductility of weld metal at elevated temperatures and the potential for high strain concentrations (both metallurgical and geometric) in the heat-affected zones of weldments, creep-fatigue evaluation in the weld region (defined as ±3 times the thickness to either side of the weld centerline) should be conducted with reduced values of the allowable number of design cycles (N_d) and allowable time duration (T_d) in Equation (18). The N_d value should be one-half that permitted for the parent material, and the T_d value should be obtained from that of the parent material by multiplying it with the weld strength reduction factor (R). The factor K' should also be used in the determination of T_d, as in the case of the base metal.

3.4.7 Creep Crack Growth and Nonductile Fracture

The code stipulates that nonductile fracture is not a problem for the approved materials at high temperatures. However, stress relaxation occurring at high temperatures may lead to high residual stresses at lower temperature where nonductile fracture is possible for ferritic alloys that show ductile-to-brittle transition behavior. The procedure discussed in Appendix G of the ASME Code or Section 3.3.5 of this report may be used to demonstrate that nonductile fracture will not occur for postulated defects. Such demonstrations are not needed for the austenitic steels or Alloy 800H.

Subsection NH does not require consideration of creep crack growth.

3.4.8 Time-Independent Buckling

Buckling limits for specific geometries under different loadings are given in Section III. These limits include the effects of geometrical imperfections permitted by fabrication tolerances on vessel shells. Subsection NH, Appendix T, lists the maximum permitted values of time-independent buckling factors as functions of Service Load Level and for load- and strain–controlled buckling. The permissible load factors are significantly larger than the permissible strain factors. However, the code does not provide any guidance for the buckling analysis except for the buckling limits for specific cases listed in Section III. It requires that the calculated load factors for load-controlled buckling and the calculated strain factors for strain-controlled buckling be less than those tabulated in Appendix T of Subsection NH.

3.4.9 Time-Dependent Buckling

Subsection NH, Appendix T, lists maximum permitted values of time-dependent, load-controlled creep buckling factors as functions of Service Load Level. These factors are a factor of two less than those used in low-temperature, load-controlled buckling. In contrast to low-temperature buckling, the factor for purely strain-controlled creep buckling is not required because strain–controlled loads are reduced concurrently with resistance of structure to buckling when creep is significant. As in the low-temperature case, the code does not provide any guidance for the creep buckling analysis. It requires that the calculated load factors for load-controlled creep buckling be less than those tabulated in Appendix T of Subsection NH.

3.4.10 Evaluation of Subsection NH

Subsection NB of the ASME Code, Section III, should be applicable to those HTGR components (e.g., pressure vessel) that will operate at relatively low temperatures. A code like Subsection NH will be needed for components (e.g., reactor internals) that will operate at high temperatures. Currently, Subsection NH provides design rules for construction of out-of-core nuclear structures fabricated from a very limited set of materials (the five materials listed in Table 3.4). However, the list of potential materials for use in the HTGR includes many other materials that are not currently in the Code. This fact alone is potentially the biggest obstacle for the use of Subsection NH as a design code for HTGRs. Although the approved list of materials for Subsection NB is larger, not all the approved materials will be suitable for service at the high temperatures (see Tables 2.2 and 2.3) where the HTGR will operate. Ferritic steel, 1Cr-0.5Mo-V, is not suitable because the maximum allowable metal temperature is low (538°C). Austenitic stainless steels, e.g., Type 304 and 316 SS, have commonly been used for high-temperature application due to their excellent strength retention at high temperatures. However, their poor thermal conductivity and relatively high thermal expansion coefficient may make them unsuitable for HTGR application.

Of the code-approved materials at present, ferritic steel, 2.25 Cr–1 Mo, may be used to fabricate the reactor core support structures and internals located in the upper portion of the vessel where the metal temperatures may be less than 500°C because of the low core inlet temperature of the coolant. Alloy 800H may be used to fabricate support structures and internals that are exposed to the maximum temperature of 760°C.

The maximum temperature permitted by Subsection NH for the materials acceptable for the HTGR core support structures is 760°C. Since the GT-MHR core support structures,

especially the ones located in the lower portion of the reactor pressure vessel, may experience temperatures of 850°C or higher, the scope of the Code Case needs to be expanded to include materials with higher allowable temperatures and other materials of interest. The candidate materials for core support structures and vessel internals include Alloy 617, 9Cr-1Mo-V steel, and Hastelloy X. Of these three materials, the database for Alloy 617 is the most complete and Section 3.7 reviews a Draft Code Case that provides design rules for Alloy 617.

A problem with using Subsection NH in the design of HTGR components is that its rules are written for materials that follow a classical creep curve, i.e., primary creep, secondary creep, and tertiary creep. However, many of the materials (e.g., Alloy 617) being considered for HTGR do not show any evidence of primary or secondary creep. New rules (such as those in the Draft Code Case for Alloy 617) have to be developed for such materials.

A significant shortcoming of Subsection NH as a design code for HTGRs is that it does not require the supporting inelastic stress analysis to be conducted with rate-dependent, high-temperature unified constitutive equations (no distinction between creep strain and plastic strain), which are necessary when components operate at very high temperatures [>649°C (1200°F)]. At such high temperatures, the tensile stress-strain curve of a material depends on the strain rate, and the classical distinction between plasticity and creep becomes untenable. Advanced unified constitutive equations are required while conducting inelastic analysis above 649°C (1200°F) with the draft code case for Alloy 617. Advanced rate-dependent unified constitutive equations will have to be developed for the candidate materials for HTGRs. As mentioned earlier, creep-fatigue damage is evaluated in Subsection NH using the time-fraction and cycle-fraction bilinear damage rule. This rule was originally developed by NASA (as linear damage rule) and was adopted by the ASME Code because of its simplicity. During the 1970s and 1980s, USDOE funded several projects to develop databases on high-temperature materials properties for the austenitic stainless steels, ferritic steel (2.25Cr-1Mo), Alloy 800H, and Alloy 718 in support of the Clinch River Breeder Reactor Program. The databases developed under the USDOE programs form a significant portion of the supporting data for the design curves (including creep and creep-fatigue) that are currently in Subsection NH. As part of the USDOE program, ANL developed the damage rate equation for predicting creep-fatigue life (Majumdar and Maiya 1980). During this time, a detailed review of the various life predictive methods was conducted by ANL (Majumdar, Maiya, and Booker 1981). The review showed that the Damage Rate Equation can account for strain rate effects, loading wave-shape effects, and various hold time effects more accurately than the linear damage rule. Since then, a review conducted by the Japanese (Muto, Miyamoto, Nakajima, and Baba 1989) has also concluded that several other life-predictive methods, including ANL's damage rate equation, can predict the creep-fatigue life of Hastelloy XR at high temperatures more accurately than the linear damage rule. The AMSE Code has continued to use the linear damage rule by changing the linear to a bilinear damage rule and adjusting the rule so that all available data are predicted conservatively. However, this leaves open the question whether the rule continues to be conservative when extrapolated significantly beyond the database. Such an extrapolation will be necessary if plants are to be designed for a 40-year life.

Subsection NH does not provide specific guidelines for environmental effects, but states that the combined effects of exposure to elevated temperature, contacting fluid, and nuclear radiation on material properties shall also be considered. Currently, there is no generally accepted method for taking environmental effects into account, because different materials behave differently in the same environment. For example, in austenitic stainless steels, tensile

holds are more damaging than compressive holds under creep-fatigue loading in air or in vacuum, because volumetric creep damage dominates failure in these materials. On the other hand, in ferritic steels (e.g., 2-1/4Cr-1Mo steel and 9Cr-1Mo steel), the converse is true, because oxidation plays a critical role in surface cracking of these alloys. Similarly under creep loading, Alloy 617 shows early surface cracking in air, but surface cracking is subdued in the He environment. The linear damage rule cannot predict such divergent behavior. Clearly, more mechanistically based predictive methods are needed to be able to handle the various material-specific damage mechanisms in different environments.

3.5 ASME B&PV Code Case N-499-1

3.5.1 Summary of Code Case N-499-1

This code case is invoked for Class 1 components fabricated from SA-533 Grade B, Cl 1 plates, as well as SA-508 Cl 3 forgings and their weldments, whose metal temperature may exceed 371°C (700°F) during Service Level B, C, and D events. The code case provides the following restrictions on the maximum temperature and allowable cumulative time at that temperature for each of the Level A, B, C, and D events.

- Metal temperature exceeding 371°C permitted only for Service Level B, C, and D events.
- Maximum temperature of 427°C (800°F) permitted for Level B events, and 538°C (1000°F) for Level C and D events.
- Maximum cumulative time of 3000 h permitted for metal temperatures between 371 and 427°C, and 1000 h for temperatures between 427 to 538°C.

The design rules of ASME Section III, Division 1, NB-3000, shall be followed for all design and operating conditions for which metal temperature does not exceed 371°C. These design rules are similar to those presented in Section 3.3, Low-Temperature Design, of this report.

The design rules of ASME Section III, Division 1, NH-2000, shall be followed for metal temperatures exceeding 427°C.

The code case provides the following physical and mechanical properties at elevated temperatures in the range of 371 to 538°C:

- Instantaneous and mean coefficients of thermal expansion,
- Moduli of elasticity,
- Yield and tensile strengths,
- Elevated temperature (538°C) fatigue strength,
- Isochronous stress-strain curves, and
- Stress-to-rupture values.

Fatigue design is based on so-called crack initiation life. Allowable fatigue cycles are determined from the design curve, shown in Figure 3.6, for smooth specimens tested. The design curve was developed by applying a factor of 2 on strain range and 20 on cycles, whichever is lower, to the mean failure curve for small polished specimens tested in air at 538°C. These factors are not safety related but are intended to account for size effect, surface finish, statistical scatter of the data, and differences between laboratory and industry environments. Miner's rule, i.e., the linear cumulative damage rule, is used to estimate total fatigue damage. There is no explicit allowance for crack growth from preexisting flaws.

The code case provides isochronous stress-strain curves to calculate the stress relaxation effect. Figure 3.7, for example, shows isochronous stress-strain curves at 538°C for the low-alloy steels considered by the code case. The code case evaluates creep-fatigue interaction using the bilinear damage summation rule, which is similar to the one shown for 2-1/4Cr–1Mo in Figure 3.5.

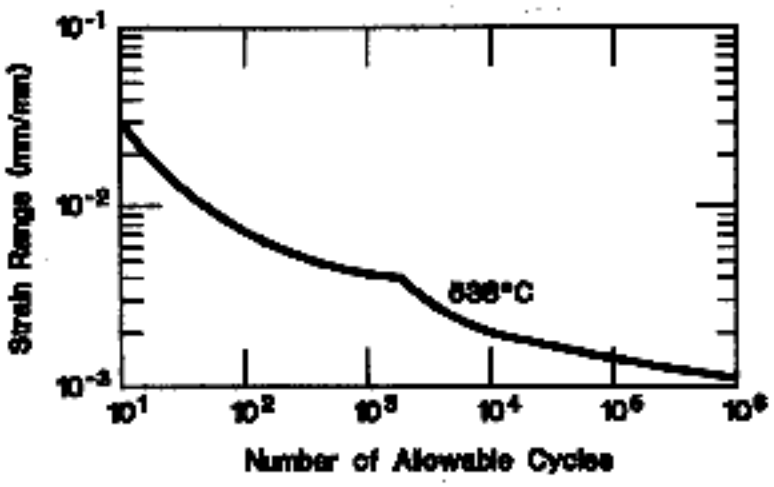

Figure 3.6. Design fatigue strain range for SA-533B Class 1 and SA-508 Class 3.

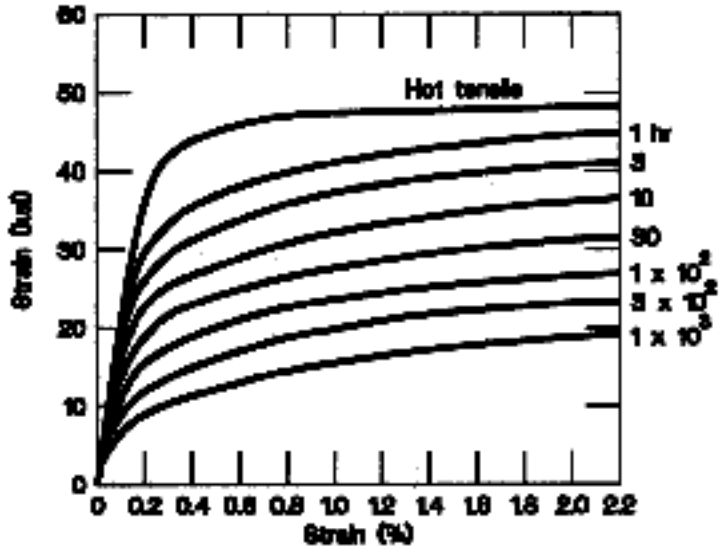

Figure 3.7. Isochronous stress-strain curves for low-alloy steels at 538°C.

3.5.2 Evaluation of Code Case N-499-1

Code Case N-499-1 may be applicable to GT-MHR reactor pressure vessel and connecting pipe made of low-alloy steels (SA 508 Cl 1, SA 533 Gr B, Cl 1) with normal operating temperature of 290°C (Service Level A conditions), provided the requirements on allowable cumulative time and maximum temperature for Service Conditions B, C, and D are satisfied. As mentioned in Table 2.3, the normal operating temperature requirement is satisfied if the vessel is insulated or cooled by helium returning from the turbine.

The scope of the code case should be expanded to include 9Cr-1Mo-V steel, which is specified for an uninsulated reactor vessel with an operating temperature of about 500°C. The code case does not address the effect of helium environment on these vessel materials. The effect of helium environment (including impurities) on the elevated-temperature (500°C) fatigue design curve, isochronous stress strain curves, stress rupture curves, and the creep-fatigue damage envelope need to be evaluated to further assess the applicability of this code case to low-alloy-steel pressure vessel materials.

3.6 ASME B&PV Code Case N-201-4

3.6.1 Summary of Code Case N-201-4

Subsection NG of ASME Section III provides rules for construction of core support structures having metal temperatures not exceeding those for which allowable stress values are given in ASME Section II, Part D. Code Case N-201-4 is invoked for core support structures that have higher metal temperatures and are fabricated from ferritic steels, austenitic stainless steels, and high-nickel alloys. The code case provides rules for construction of core support structures in two parts, Part A and Part B. Part A extends the rules for construction of Subsection NG for restricted service at elevated temperature without explicit consideration of creep and stress-rupture, whereas Part B alters the rules for service at elevated temperature by accounting for both creep and stress rupture effects. As a result, the highest temperatures permitted by Part A are lower than those by Part B. Table 3.2 lists the materials included in the code case, the maximum temperatures permitted by Subsection NG, and those permitted

Table 3.2. Maximum allowable temperatures for the materials included in Code Case N-201-4

Materials	Maximum Allowable Metal Temperatures, °C		
	Subsection NG, ASME Section III	Code Case 201-4	
		Part A[1]	Part B[2]
304 SS	538	538	816
316 Ss	538	593	816
Alloy 800H	427	649	760
2.25Cr - 1Mo	371	593	593[3]
1Cr-0.5Mo-V	371	538	Not Permitted

[1]These maximum metal temperatures are allowed provided the time and temperature requirements of Appendix XIX, Part A of the code case are satisfied.
[2]Maximum allowable time is 300,000 hours.
[3]Higher temperature (649°C) is allowed for the maximum allowable time of 1,000 hours.

by Parts A and B of this code case. Note that the materials included in the code case are the same as those included in Subsection NH (see Section 3.4 of the report), except the code case does not include the bolting material Alloy 718. Also note that the maximum temperatures and corresponding exposure times permitted by Part B of the Code are the same as those permitted by Subsection NH.

This section focuses on the review of Part B because most of the core support structure components in the high-temperature gas cooled reactors have normal operating temperatures in the range of 500-950°C. Part B considers the time-dependent material properties and structural behavior for protecting against the following four failure modes:

(a) Ductile rupture from short-term loadings,

(b) Creep rupture from long-term loading,

(c) Gross distortion due to incremental collapse and ratcheting, and

(d) Creep-fatigue failure.

Part B of the code case also provides brief guidelines for the following three failure modes:

(e) Loss of function due to excessive deformation,

(f) Buckling due to short-term loadings, and

(g) Creep buckling due to long-term loading.

The above failure modes include two time-independent failure modes [Modes (a) and (f)], and the remaining are time-dependent modes. The time-independent modes are similar to Failure Modes (1) and (3) identified in Section 3.3. The time-dependent modes are similar to the ones identified in Section 3.4, except they do not include a failure due to creep growth and non-ductile fracture.

The code case provides mandatory design rules and limits for load-controlled stresses in structures for protecting against the first two failure modes [i.e., Failure Modes (a) and (b)]. For the remaining five failure modes, the code case provides nonmandatory design rules and limits on deformation-controlled quantities (i.e., strain, deformation, and fatigue) at elevated temperatures. The design rules are similar to those presented in Sections 3.4 and 3.5 of this report, and therefore are not presented here. Note that this code case does not differentiate between general and local primary membrane stress. Therefore, the term P_L (local primary membrane stress) in the design rules in Sections 3.4 and 3.5 should be replaced by the term P_m when those rules are applied to this code case.

The code case does not provide specific guidelines for environmental effects, but states that the combined effects of exposure to elevated temperature, contacting fluid, and nuclear radiation on material properties shall also be considered.

3.6.2 Evaluation of Code Case N-201-4

This code case provides design rules for construction of core support structures fabricated from the five materials listed in Table 3.2. Some of these materials are not suitable for the high temperature (See Tables 2.2 and 2.3) and radiation environment to which the HTGR core support structures will be exposed. Ferritic steel, 1Cr-0.5Mo-V, is not suitable because the maximum allowable metal temperature is low (538°C), and its use is not permitted by Part B of the code case, which accounts for both creep and stress rupture effects. Austenitic stainless steels, e.g., Types 304 and 316 SS, have commonly been used for high-temperature steam application due to their excellent strength retention at high temperatures. However, the database is not sufficient for use of these alloys at 600°C and higher in the impure helium environment of HTGRs. Furthermore, the austenitic stainless steels exhibit high thermal expansion rates and low thermal conductivity. This results in the development of high thermally induced stresses during heating and cooling, which can cause thermal fatigue and creep.

Ferritic steel, 2.25 Cr–1 Mo, may be used to fabricate the reactor core support structures and internals located in the upper portion of the vessel where the metal temperatures may be less than 500°C because of the low core inlet temperature of the coolant. Alloy 800H may be used to fabricate the support structures and internals that are exposed to the maximum temperature of 760°C.

The maximum temperature permitted by this code case for the materials acceptable for the HTGR core support structures is 760°C. Since the GT-MHR core support structures, especially the ones located in the lower portion of the reactor pressure vessel, may experience temperatures of 850°C or higher, the scope of the code case needs to be expanded to include materials with higher allowable temperatures. The candidate materials for core support structures and vessel internals are Alloy 617 and 9Cr-1Mo-V steel. Section 3.7 reviews a draft code case that provides design rules for Alloy 617. Design rules for 9Cr-1Mo-V steel need to be developed. Note that this material has been codified in the RCC-MR code (Chellapandi, Ramesh, Chetal, and Bhoje 1996).

The code case does not provide specific guidelines for environmental effects, but states that the combined effects of exposure to elevated temperature, contacting fluid, and nuclear radiation on material properties shall also be considered. Therefore, the effects of helium coolant and nuclear radiation on the material properties of Alloy 800H and 2.25Cr-1Mo steel needs to be evaluated. In addition, the effect of helium coolant and nuclear radiation on creep and creep fatigue behavior of these two materials needs to be evaluated. Natesen, Purohit, and Tam (2003) have presented in a companion report some of the available test results showing the effects of impure helium environment on the material properties of Alloy 800H and 2.25Cr-1Mo steel. These data need to be evaluated for developing the corresponding design guidelines.

3.7 ASME B&PV Draft Code Case for Alloy 617[2]

Very-high-temperature reactors (VHTRs) are an important extension of GT-MHRs, which are becoming VHTRs as the reactor outlet coolant temperature is increased. The higher outlet temperature permits practical application of the gas-turbine Brayton cycle; it can also provide for process heat. Potential process heat applications include, for example, steam reforming of methane, steam gasification of coal, and alumina production from bauxite. Reactor outlet coolant temperatures of about 950°C are needed for each of these applications. The original request to the ASME Boiler and Pressure Vessel Code Committee for design rules for VHTR components came from the U.S. Department of Energy and one of its contractors. The specific VHTR component of primary interest was a steam-methane reformer, which would be a part of the reactor coolant primary pressure boundary and would operate at temperatures of 950°C or less. Materials of potential interest included nickel alloys 800H, X, and 617. An ad hoc task force of the ASME Code was established in 1983 to address the design of reactors operating at very high temperatures. The name of the group was the Task Force on Very-High Temperature Design. The Task Force consisted of J. M. Corum, A. W. Dalcher (Chairman), C. W. Lawton, R. I. Jetter, D. I. Roberts, and S. Yukawa. T. Kondo of JAERI (Japan) and F. Shubert of KFA (Germany) also participated. The task force was organized under the jurisdiction of the Subgroup on Elevated Temperature Design of the Subcommittee on Design. The Task Force completed the draft code case in 1989 and submitted it to the Subgroup, which later approved the code case. No further work was done on the draft code case because of the reduced interest from USDOE and its contractor.

The draft code case was patterned after relevant portions of Code Case N-47, and limited to Alloy 617, temperature of 982°C (1800°F), and maximum service life [total life at temperatures above 427°C (800°F)] of 100,000 h or less. The draft code case focused on Alloy 617 because it was a leading candidate of designers, and there was a significant material properties database at the temperature of interest. The code case focused on all the failure modes listed in Sections 3.3 and 3.4, including nonductile failure. The last failure mode was considered because of the significant loss of fracture toughness in Alloy 617 after long-term exposure to high temperatures.

3.7.1 Draft Code Case Features

Most of the design rules addressed by the draft code case are similar to those provided by Subsection NH discussed in Section 3.4. Some design rules are different from the Subsection NH rules because the draft code case considers higher temperature and different material. These differences, as well as several other points about the draft case, are summarized here.

At the very high temperatures of interest Alloy 617 exhibits unique material behavior that must be accounted for in the design rules. This behavior includes (1) lack of clear distinction between time-independent and time-dependent behavior, (2) high dependence of flow stress on strain rate, and (3) softening with time, temperature, and strain. Therefore, the design rules of Subsection NH that are based on time- and rate-independent, or strain-hardening idealizations

[2]This Section summarizes the information presented by Corum and Blass (1991). Other references are identified as appropriate.

of material behavior required careful consideration in the draft case. For example, the case specifies that inelastic design analyses for temperatures above 649°C (1200°F) must be based on unified constitutive equations, which do not distinguish between time-independent plasticity and time-dependent creep.

The draft case recognizes that significant environmental effects on Alloy 617 behavior could exist in VHTRs. The helium coolant will generally contain some hydrogen, water vapor, carbon monoxide, carbon dioxide, methane, and nitrogen. There is potential for oxidation and carburization or decarburization of metals exposed to the coolant. Rapid carburization or decarburization can occur above 482°C (900°F). However, the Task Force for the draft case believed that carburization of Alloy 617 can be limited to acceptable values for the temperatures covered. The draft case states that its design rules are applicable provided the coolant does not influence component behavior to a greater extent than air. Some results for the effect of impure helium environment on fatigue behavior of Alloy 617 are presented by Natesen, Purohit, and Tam (2003). These data need to be evaluated for developing the corresponding design guidelines.

Extended exposure at elevated temperature may cause a significant reduction in fracture toughness of Alloy 617. The draft case requires a fracture mechanics analysis to justify the ability of the component to withstand the expected service conditions, especially when the component cools down to lower temperatures. Because of the concern for potential loss of fracture toughness, Alloy 617 bolting is excluded from the draft Case. In addition, exposure of cold-worked material to very high temperatures results in recrystallization. Therefore, cold-worked Alloy 617 is also excluded from the draft case.

Whereas Subsection NH is limited to 300,000 h, the draft case is limited to design lives of 100,000 h or less. The main reasons for this shorter design life are (1) the uncertainties of data extrapolation at very high temperatures, and (2) at long times, the allowable stresses are less than 1 ksi at the highest temperatures; there is lack of experience in designing reliably at such low allowable stresses.

The allowable stress quantities used in Subsection NH are S_0, S_m, S_t, and S_{mt} as defined in Sections 3.3 and 3.4. These quantities are retained in the draft case. However, the basis for S_t, the time-dependent allowable stress, was altered slightly so that it does not depend on tertiary creep.

Another difference between draft case and Subsection NH is in the Level D Service Limits. In Subsection NH, the Level D Service Limits are obtained in part from Appendix F of Section III as mentioned in Section 3.4.3. In the draft case, the limits from the Appendix are replaced by 70% of the lesser of the collapse load and the plastic instability load. The draft case cautions that problems can arise from material instability associated with strain softening, as well as structural instability.

3.7.2 Allowable Stress and Stress Rupture Values

In the draft case, limits are placed on load-controlled (primary) stresses that are obtained from elastic analysis. The limits are based on values of S_{mt}, S_m, S_t, and S_r. These values are determined using the following criteria:

$$S_{mt} = \min \begin{cases} S_m \\ S_t \end{cases} \tag{24}$$

$$S_m = \min \begin{cases} 1/3 \text{ specified minimum UTS at RT} \\ 11/30 \text{ minimum UTS at temperature} \\ 2/3 \text{ specified minimum } S_y \text{ at RT} \\ 90\% \text{ minimum } S_y \text{ at temperature upto 649°C (1200°F)} \\ 2/3 \text{ minimum } S_y \text{ above 649°C (1200°F)} \end{cases} \tag{25a}$$

$$S_t = \min \begin{cases} 2/3 \text{ minimum stress to rupture in time t} \\ \text{Minimum stress to produce 1\% strain in time t} \end{cases} \tag{25b}$$

$$S_r = \text{minimum stress to rupture} \tag{25c}$$

The above criteria are similar to those employed for Subsection NH with some exceptions. The criteria for S_t do not include 80% of minimum stress for onset of tertiary creep because an increasing strain rate is observed very early in constant-load creep tests of Alloy 617 at temperatures close to 982°C. Also, two fractions of the yield strength are used in the S_m definition because the shape of the stress-strain curve changes in going from high temperature to very high temperatures. Figure 3.8 is a plot of S_m and S_t for given times versus temperature. Figure 3.9 is a plot of S_t versus time for given temperatures. Figure 3.10 is a plot of S_r versus time for given temperatures.

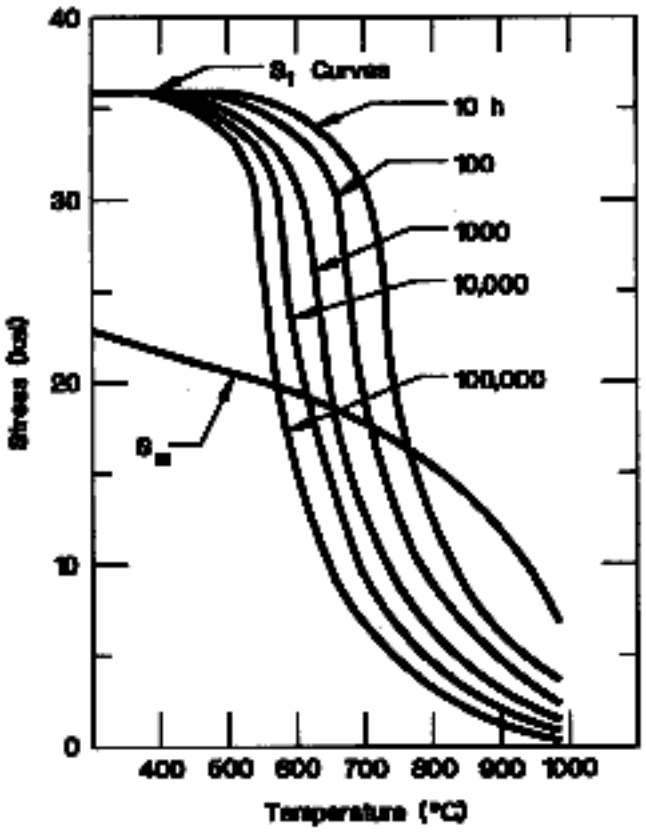

Figure 3.8. S_m and S_t for given times vs temperature for Alloy 617 (Corum and Blass 1991).

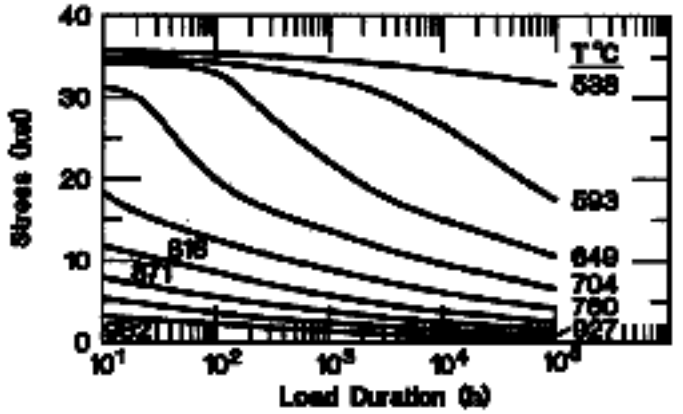

Figure 3.9. S_t vs time for given temperature for Alloy 617 (Corum and Blass 1991).

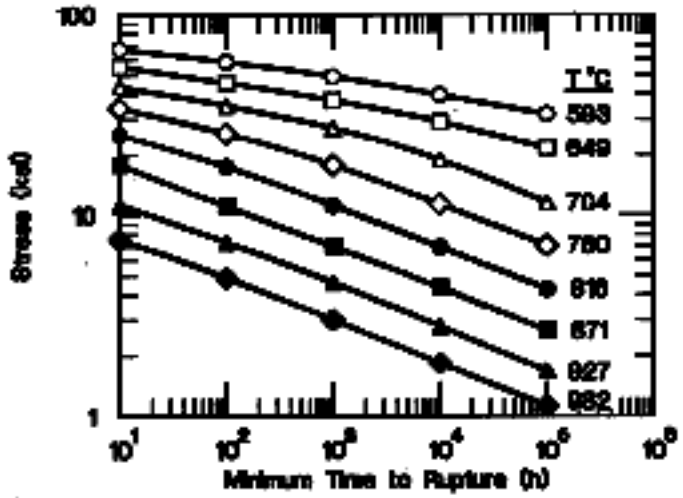

Figure 3.10. S_r vs time for given temperature for Alloy 617 (Corum and Blass 1991).

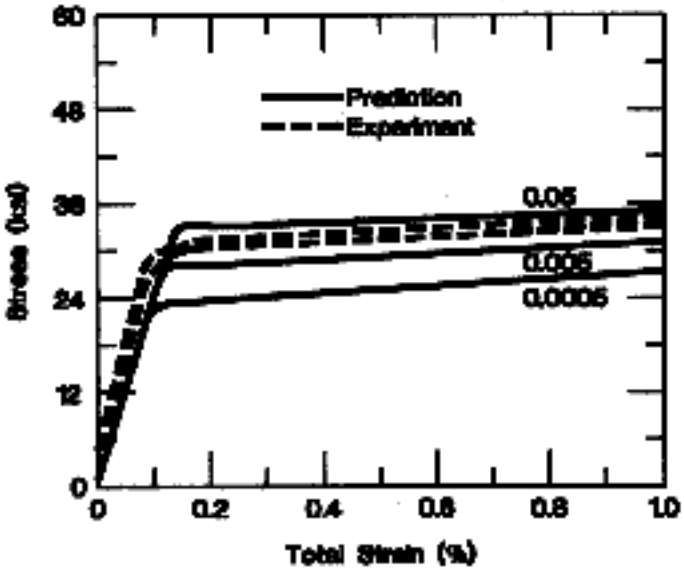

Figure 3.11. Calculated and observed stress vs strain for Alloy 617 at 750°C given strain rates (per min) (Corum and Blass 1991).

3.7.3 Unified Constitutive Model and Isochronous Stress-Strain Curves

Constitutive models of inelastic behavior are typically based on classical concepts of time-independent plasticity and time-dependent creep. In such models, inelastic strain is considered to be a sum of separately evaluated plastic and creep strain. However, for Alloy 617

at temperatures close to 982°C, this distinction between plasticity and creep is unrealistic; inelastic behavior is always significantly time or rate dependent. Therefore, the draft code case employs a so-called unified constitutive model, which was developed by Robinson (1984) at ORNL. This model can provide a useful description of both short- and long-term behavior as a function of loading rate. Figures 3.11 and 3.12 provide comparisons of experimental and analytical results for typical tensile loading conditions, respectively, at 750 and 950°C. Figure 3.13 provides similar comparisons for creep loading conditions.

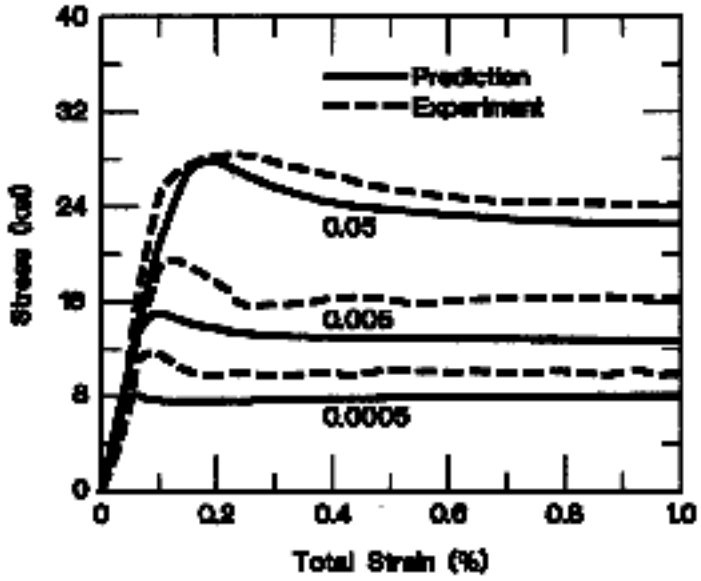

Figure 3.12. Calculated and observed stress vs strain for Alloy 617 at 950°C for given strain rates (per min) (Corum and Blass 1991).

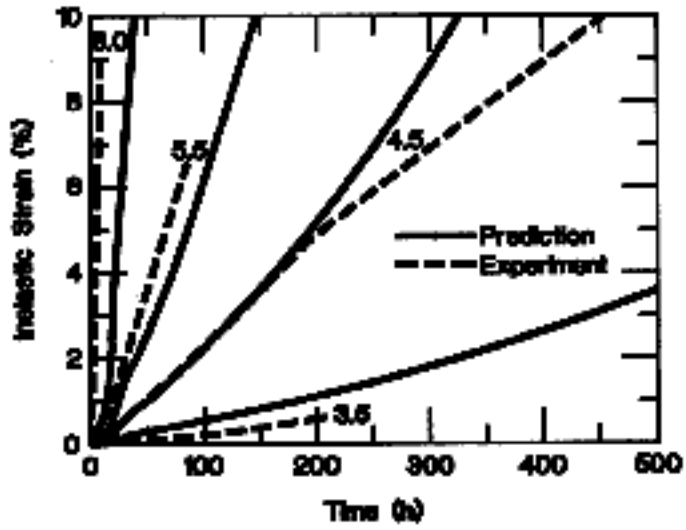

Figure 3.13. Calculated and observed strain vs time for Alloy 617 at 950°C for given stresses (in ksi) (Corum and Blass 1991).

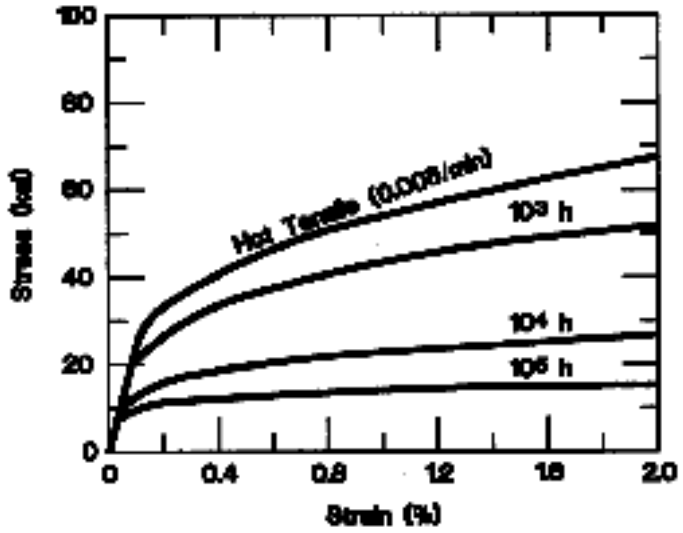

Figure 3.14. Average isochronous stress vs strain for Alloy 617 at 649°C at given times (Corum and Blass 1991).

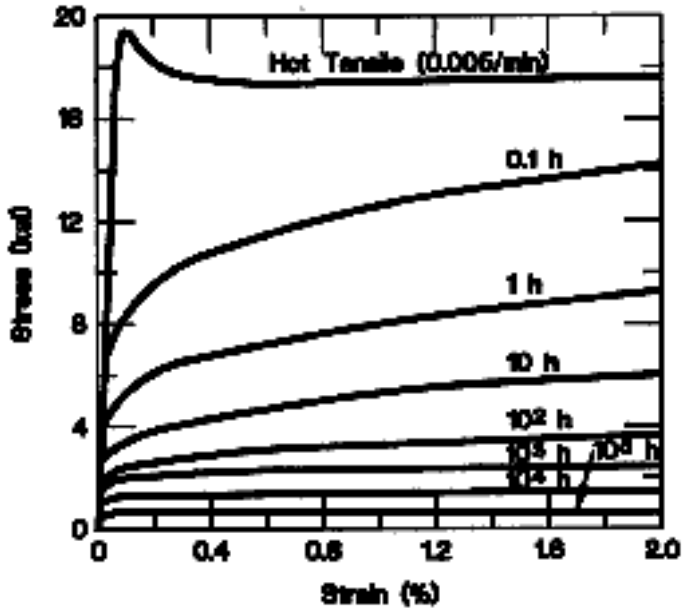

Figure 3.15. Average isochronous stress vs strain for Alloy 617 at 982°C for given times (Corum and Blass 1991).

The unified model was used to generate isochronous curves of stress versus strain. These curves were then modified to match the average behavior of Alloy 617. This was accomplished by matching the average values of 0.2% offset yield strength and stress to produce 1% creep strain in a given time for Alloy 617. Figures 3.14 and 3.15, respectively, show the average isochronous stress versus strain at 649 and 982°C at given times.

3.7.4 High-Temperature Limits for Cyclic Loading

Yukawa (1991) describes the formulation of fatigue design curves that are included in the draft code case. The draft case is based on air-environment material properties, including fatigue. The data selected for formulation of the design curves were from fatigue tests on five heats of Alloy 617 in the temperature range of 538 to 1000°C. The selected data also include fatigue test results at 1000°C for three grain sizes. All of these data are for axially loaded test specimens, and most of the testing in the low-cycle range was done at a nominal strain rate of 4×10^{-3}/s.

The analysis of the fatigue data was done using the following generalized equation:

$$\Delta\varepsilon_t = A(N_f)^a + B(N_f)^b \quad (26)$$

where

$\Delta\varepsilon_t$ = total strain range

N_f = number of cycles to failures

A, a, B, b = fitted coefficients and exponents

In Equation (26), the first term on the right side is the inelastic portion of the total strain range, and the second term is the elastic portion. The coefficients and exponents in Equation (26) were determined by regression analysis. The values of the coefficient and exponent (A and a) were found to be independent of temperature in the range of 538 to 927°C. The values of the coefficient and exponent for the elastic strain component were found to be dependent on temperature. For analysis purposes, this temperature effect was divided into three groups, and three corresponding sets of values of B and b were determined.

Two additional steps were taken to derive design fatigue curves from the best-fit equation. One step involves a Poisson's ratio adjustment, and the second involves the incorporation of design margins. Manson's (1966) method was used to adjust for the Poisson's ratio between the elastic and plastic conditions. This involves reducing the elastic strain part of Equation (26) by a factor equal to $(2/3)(1+\nu)$, where ν is elastic Poisson's ratio.

The design margins were incorporated using a procedure proposed by Manjoine and Johnson (1986). This procedure is similar to the usual code method of applying a factor of 2 on stress and a factor of 20 on cyclic life, but it avoids the "cusp" that sometimes occurs in the design curve. The Manjoine and Johnson procedure uses an equation of the following form:

$$\varepsilon_d = m_p\varepsilon_p + m_e\varepsilon_e \quad (27)$$

where ε_d is the design allowable total strain range, and ε_p and ε_e are the plastic and elastic strain range, respectively. The factors m_p and m_e are reduction factors for the plastic and elastic strain ranges, and their values correspond to 20 on cycles and 2 on stress in the usual code procedure. The factor m_p is equal to 20^a, where "a" is the exponent in Equation (26), and m_e equals 0.5.

Applying the Poisson's adjustment and the design margins using the Manjoine and Johnson procedure produces the following fatigue design equation:

$$\varepsilon_t = [0.103A(N_d)^a + 0.5(2/3)(1 + 0.3)B(N_d)^b]/100 \quad (28)$$

where the value of 0.103 equals m_p and is obtained from 20^a with a = -0.76. N_d is the number of allowable cycles, and ε_t is used to denote the design fatigue strain range. The resulting fatigue design curves are shown in Figure 3.16.

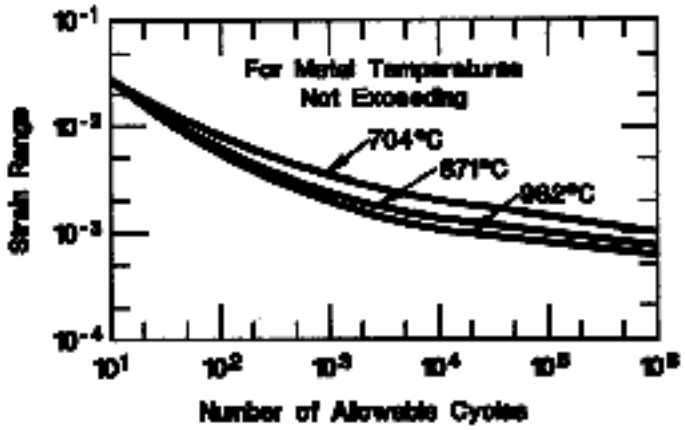

Figure 3.16. Design fatigue strain, ε_t, for Alloy 617 (Yukuwa 1991).

As mentioned, the draft code case is based on materials tested in an air environment. The case contains a provision that it should be determined whether the operating fluid does affect component behavior to a greater extent than air. However, in helium cooled reactors, the helium could contain a small amount of impurities that, at high temperatures, could be oxidizing, reducing, carburizing, or decarburizing to metallic alloys, including Alloy 617. A number of fatigue tests (Strizak et al. 1982) and other mechanical property tests have been done in helium containing a small amount of impurity gases, and details are presented in a companion report (Natesan, Purohit, and Tam 2003).

3.7.5 High-Temperature Ratcheting Limits

The draft code case imposes inelastic strain limits for base metal and weld metal that are similar to the limits given in Subsection NH and presented in Section 3.4.5 of this report. The draft case follows the elastic and inelastic analysis rules of Subsection NH, but an upper temperature limitation of 649°C is imposed on their applicability. The main reason for this limitation is that below this temperature, Alloy 617 behavior is qualitatively similar to that of other materials for which creep ratcheting has been well studied and the rules validated. Above 649°C, the behavior of Alloy 617 is different as discussed, and validated and simplified ratcheting analysis procedures do not exist.

3.7.6 High-Temperature Creep-Fatigue Rule

The creep-fatigue evaluation procedures adopted by the draft code case are similar to the ones in Subsection NH and discussed in Section 3.4.6 of this report. The creep-fatigue damage envelope for both elastic and inelastic rules is similar to the one for Alloy 800H shown in Figure 3.5. Natesan, Purohit, and Tam (2003) present some results on the environmental effects of impure helium on creep-fatigue behavior of Alloy 617 in the companion report.

3.7.7 Buckling Rules

At temperatures below 649°C, the buckling rules are similar to the ones in Subsection NH as described in Sections 3.4.8 and 3.4.9 of this report. For temperatures above 649°C, the draft case specifies that unified constitutive equations must be used in calculating buckling loads, whether to meet the limits for time-independent or time-dependent buckling.

3.7.8 Evaluation of the Draft Code Case

The draft code case is based on limited available information on Alloy 617 and experience with the application of that alloy. Corum and Blass (1991) have formulated recommendations for the further development of the draft case before it could be satisfactorily and reliably applied. These recommendations are presented below in three categories.

Actions Required in Code Case Area:

- Alloy 617 must be added to the low-temperature rules of Section III.
- Weldment stress rupture factors must be added.
- Thermal expansion coefficient must be added.
- Additional isochronous stress-strain curves covering the temperature range from 427°C to 649°C must be added.

Material Data Needs:

- Weldment fatigue data are needed.
- More complete creep-fatigue database is needed.
- The synergistic effects of aging, environment, loading, and temperature should be better understood.
- The effects of aging on toughness must be characterized.

Structural Design Methodology Needs:

- The unified constitutive model included in the draft case is based just on uniaxial tensile and creep data. Although this model is adequate for generating isochronous stress-strain curves, more complete, experimentally based equations need to be developed for design analysis use.
- Some very-high-temperature, time-dependent tests of Alloy 617 structural models are needed to (1) provide better understanding of structural behavior and failure modes, and (2) validate inelastic analysis methods and failure modes.
- Simplified ratcheting evaluation procedures need to be developed for temperatures above 649°C.
- The use of linear damage fractions as the basis of the creep-fatigue rules is probably the biggest shortcoming of the draft case. This is discussed in Section 6.3. A basic effort is needed to identify and experimentally validate a more suitable damage theory.

4 RCC-MR, Design and Construction Rules for Mechanical Components of FBR Nuclear Islands (French Code)

The French high-temperature code RCC-MR is an extension of the low-temperature code RCC-M. Both codes have rules that are similar to the ASME Code rules. However, the RCC-MR rules are organized according to the damages that are possible at high temperature, which is a little different from how the ASME Code is organized. RCC-MR distinguishes between two broad types of possible damages, P type and S type. The P type damages result from the application of a steadily increasing load or constant load. The S type damages occur due to repeated application of loading. The P type damages include immediate excessive deformation, immediate plastic instability, time-dependent excessive deformation, time-dependent plastic instability, time-dependent fracture, and elastic or elastoplastic instability. The S type damages include progressive deformation and fatigue or progressive cracking. Most of the design rules contained in RCC-MR are very similar to those in the ASME Code. As in the ASME Code, both elastic analysis rules and elastoplastic analysis rules are provided. Therefore, we will concentrate our discussions mainly in those areas where there are differences.

As in the ASME Code, RCC-MR contains criteria for Service Load Levels A, C, and D, but Service Load Level B is absent in RCC-MR. The classification of stresses into primary and secondary, and into membrane, bending, and peak is identical to the ASME Code. To handle multiaxial stresses, RCC-MR allows the use of either the maximum shear theory (Tresca) or octahedral shear theory to compute stress intensities or stress range intensities.

The primary membrane and membrane-plus-bending stress allowables at low and high temperatures in RCC-MR are basically the same as those in the ASME Code, Section III, Subsection NH. However, the rules are cast in terms of creep and creep rupture usage fractions rather than S_m, S_t, and S_{mt} as in the ASME Code.

To prevent progressive deformation in the low-temperature regime, RCC-MR allows the use of either the $3S_m$ rule or a rule based on an efficiency diagram. The $3S_m$ rule is basically the same as in Subsection NB. The efficiency diagram is used to convert a steady primary stress and a cyclic secondary stress range into an effective primary stress that will produce the same deformation as the combined steady primary and cyclic secondary stresses. To define the effective primary stress, a secondary ratio SR is defined as the ratio between the secondary stress intensity range and the maximum primary membrane stress intensity,

$$SR_1 = \frac{\Delta Q}{\mathrm{Max}(P_m)} \tag{29a}$$

A similar ratio using the maximum local membrane-plus-bending stress intensity is also defined,

$$SR_2 = \frac{\Delta Q}{\mathrm{Max}(P_L + P_b)} \tag{29b}$$

For each of the above two secondary ratios, an efficiency index (v) is obtained from an efficiency diagram, which is equivalent to the following equation:

$$v = \begin{cases} 1 \text{ for } SR \le 0.46 \\ 1.093 - 0.926 SR^2 / (1 + SR)^2 \text{ for } 0.46 \le SR < 4 \\ 1/\sqrt{SR} \text{ for } SR \ge 4 \end{cases} \quad (30)$$

The effective primary stress intensities are then defined as follows:

$$P_1 = \text{Max } P_m / v_1 \quad (31a)$$

and

$$P_2 = \text{Max } (P_L + P_b)/v_2 \quad (31b)$$

To prevent ratcheting, P_1 has to be limited as a primary stress. Requiring $P_1 \le S_m$ would ensure the same safety margin with and without progressive deformation. However, in RCC-MR, the safety margin has been reduced for the case of progressive deformation by limiting P_1 to 1.2 S_m (~S_y for austenitic stainless steels), which leads to the following Level A criterion for P_1:

$$P_1 \le 1.2\ S_m \quad (32a)$$

In a similar fashion, P_2 for the Level A criterion is limited as follows:

$$P_2 \le 1.2 \text{ x } 1.5 S_m \quad (32b)$$

RCC-MR gives a rather elaborate step by step procedure for evaluating the fatigue usage fraction, which is quite similar (but not identical) to that of Subsection NH. The elastically calculated strain ranges are amplified due to plasticity by using a variation of Neuber's equation and a special treatment for any primary stress range that could lead to a similar amplification.

RCC-MR does consider the possibility of the presence of zones containing geometrical discontinuities. No fatigue analysis is required for material located at a distance less than a characteristic distance d from the discontinuity. Fatigue analysis is required for materials beyond the characteristic distance d, where for materials with maximum specified ultimate tensile strength at room temperature less than 600 MPa, d = 0.05 mm.

At high temperatures, RCC-MR uses the same efficiency diagram as discussed in the low-temperature ratcheting section [i.e., Equation (30)], with the exception that, instead of P_2, the effective primary stress intensity for membrane-plus-bending stress corrected by the creep bending shape factor P_3 is defined as follows:

$$P_3 = \text{Max } (P_L + \varphi P_b)/v_3 \quad (33a)$$

where φ is the creep bending shape factor (same as $1/K_t$ in Subsection NH), and v_3 is determined from the efficiency diagram corresponding to

$$SR_3 = \frac{\Delta Q}{\text{Max}(P_L + \varphi P_b)} \quad (33b)$$

Both P_1 and P_3 are limited by limiting the creep usage fractions corresponding to $P_1/1.2$ and $P_3/1.2$ to 1.0.

At high temperatures, RCC-MR uses a creep-fatigue interaction rule based on the summation of cycle fraction fatigue damage and time-fraction (linear damage rule) creep damage. This rule is very similar to that used in Subsection NH, with the exception that an octahedral shear or Tresca criterion is used for computing effective stress rather than Equation (22). The strain range is amplified to account for plasticity and creep effects in a slightly different fashion than Subsection NH, and the effective stress is divided by a factor of 0.9 (rather than 0.67 as in Subsection NH) before computing the creep damage.

4.1 Background Information on Efficiency Diagram

The efficiency diagram has been developed on the basis of tests on a large variety of specimen geometry and loading, including non-axisymmetrical ones (Autrusson 1988)::

- Three bar assemblies, with constant load and different cyclically varying temperatures between the central and the lateral bars,
- metal band with applied weight and cyclically varying curvature,
- tension-torsion,
- test on components, such as piping, under thermal shocks,

as well as on different materials (ferritic steel, austenitic steel, other steels, and Incoloy 800), and test temperatures (from room temperature to 650°C). Each test is characterized by the efficiency index (v) and the secondary ratio (SR):

$$v = \frac{P}{P_{eff}} \tag{34a}$$

$$SR = \frac{\Delta Q}{P} \tag{34b}$$

The test results are plotted with secondary ratio, SR, along the x axis and the efficiency index, v, along the y axis. The results showed scatter, which occurs largely due to difficulty in estimating the stabilized cumulative starin (after sufficient number of cycles) and material characteristics (especially the stress-strain curves). The lower bound to these data represents the efficiency diagram. For application to codes and standards, P_{eff} is determined from a lower bound to all experimental data leading to the functional relationship between SR and v given in Equation (30).

4.2 Comparison between Efficiency Diagram and the Bree Diagram

The Bree diagram can be plotted in the efficiency diagram coordinates by first transforming the Bree diagram limit [Equation (5b)] to give (after noting that $S_y \approx 1.2S_m$ for stainless steels) the following for the primary membrane:

$$G(SR_1) \geq v_1 = \frac{\bar{P}_m}{1.2\,S_m} \tag{35a}$$

where

$$G(SR_1) = \begin{cases} \dfrac{1}{\sqrt{SR_1}} & \text{for } SR_1 \geq 4 \\ \dfrac{4}{4 + SR_1} & \text{for } 4 \geq SR_1 \geq 0 \end{cases} \qquad (35b)$$

A similar transformation can be used for the primary membrane-plus-bending case.

A comparison between the efficiency diagram [Equation (30)] and the Bree diagram transformed to the new coordinate system [Equation (5b)] with K=1.5 is shown in Figure 4.1 for several loadings. Except at low values of SR_1, the two plots coincide with each other for the case of general membrane loading (P_m), which is to be expected from a comparison between Equations (5b) and (35b). The curve for pure bending and the local primary membrane falls below the curves for the general primary membrane. The curve for the local primary membrane-plus-bending loading with $P_L = P_b$ falls between those for the pure bending and the pure membrane loading cases, as expected. Note that all the transformed Bree diagrams fall below the efficiency diagram of RCC-MR and are generally also lower than the lower bound used to justify the RCC-MR curve. Thus, the Bree diagrams, transformed to the efficiency diagram coordinate system, provide lower bounds not only to the efficiency diagram of RCC-MR but also to the test data used in the development of the RCC-MR approach. The same general trends are also observed if the efficiency diagram is transformed to the Bree diagram coordinate system and superimposed on the Bree diagram.

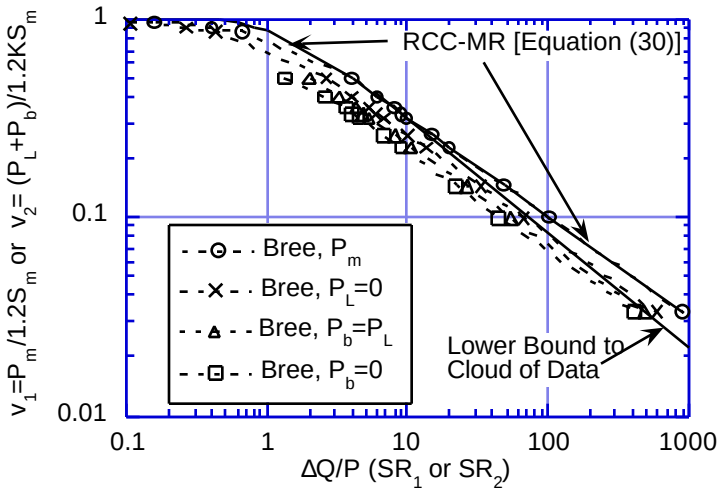

Figure 4.1. Comparison of the RCC-MR efficiency diagram with those calculated from Bree diagram analyses.

4.3 Evaluation of RCC-MR Code

RCC-MR was developed in France as a high-temperature extension to RCC-M, for the French breeder reactor program. The basic rules in RCC-MR are very similar to those in ASME Code Subsection NH. RCC-MR provides more detailed instructions on how to carry out fatigue and creep-fatigue design analysis than the ASME Codes. It also uses a somewhat different approach to analyzing creep ratcheting without the use of isochronous stress-strain curves. But the basic safety factors used in generating the design curves in the two codes are

comparable. The choice of materials in RCC-MR is also limited; however, modified 9Cr-1Mo is codified in RCC-MR (Chellapandi, Ramesh, Chetal, and Bhoje 1996).

5.0 Procedure R5, Assessment Procedure for the High-Temperature Response of Structures (British Procedure)

Procedure R5 involves a comprehensive assessment of the high-temperature response of structures. The procedure addresses the following aspects of high-temperature behavior (Goodall and Ainsworth 1991):

- Simplified methods of stress analysis
- Creep-fatigue crack initiation
- Creep crack growth
- Creep-fatigue crack growth
- Behavior of dissimilar metal welds
- Behavior of similar metal welds

The main objective of the procedure is to ensure that failure of the defect-free and defective component by creep rupture is avoided. The calculation of the expected lifetime is generally performed by conservative approximations based on Reference Stress Techniques. The remaining life at any time, t, cannot exceed

$$t_r\,[\sigma_{ref}(t)] \tag{36}$$

where t_r is the rupture time from uniaxial stress/time-to-rupture data, and $\sigma_{ref}(t)$ is the reference stress calculated using the crack size, a(t):

$$\sigma_{ref}(t) = P\sigma_y / P_L[\sigma_y, a(t)] \tag{37}$$

where P_L is the limit load for the cracked geometry for a yield stress σ_y, and P is the applied load. Thus, the use of the reference stress concept allows one to estimate the remaining life of a component under given loading from the results of a single uniaxial creep test performed at the reference stress at that loading. Determination of the reference stress by Equation (37) requires an accurate limit load solution. Reference stress methods are now used in estimating creep deformations, rupture times, and the creep-cracking behavior of components. They form the basis for Procedure R5 (Penny and Marriott 1995).

5.1 Creep Crack Growth Assessment

The procedure gives the following relation for steady-state creep crack growth, $\dot{a}$:

$$\dot{a} = A(C^*)^q \tag{38}$$

where *A* and *q* are experimentally determined material constants. The constant *A* is inversely proportional to the material ductility. Under cyclic loading, the constants *A* and *q* are often weakly dependent on hold time. The above form of equation for creep crack growth has been confirmed by experiment and leads to a straight line on a log-log plot (Ainsworth, Ruggles, and Takahashi 1992; Goodall and Ainsworth 1991).

The parameter C^* controls the crack growth, and it is the counterpart of J integral in the assessment of low-temperature fracture. The value of C^* for both steady state and cyclic loading can be estimated by

$$C^* = \sigma_{ref}\, \varepsilon_{ref}\, R' \tag{39}$$

where ε_{ref} is the strain rate at the reference stress, and R' is a length scale, which depends only on the geometry of the component, $R' = K^2/(\sigma_{ref})^2$, e.g., for a crack in an infinite plate, $R' = \pi a$.

5.2 Creep-Fatigue Evaluation

The R5 procedure permits use of ductility exhaustion for creep-fatigue evaluation, if the material data are available. If appropriate data are not available, a linear damage summation similar to that recommended by ASME Code Subsection NH (Section 3.4) is used (Penny and Marriott 1995).

The R5 procedure for the evaluation of component failure due to creep-fatigue is different from that in Subsection NH and RCC-MR code. It does not consider the end of the creep-fatigue life to be indicative of component failure but merely the initiation of a macroscopic crack. It then assesses the time for the crack to grow to a critical size, using the simplified C^* approach outlined in Section 5.1, to predict crack propagation during hold periods, and a Paris Law type relationship for the cyclic growth during rapid transients, that is,

$$\left.\frac{da}{dt}\right|_{cycle} = \left.\frac{da}{dN}\right|_{transient} + \left.\frac{da}{dt}\right|_{hold} \tag{40}$$

Crack growth using Equation (40) must be determined for each cycle type. The total crack extension or remaining life can be determined by summing the crack growth per cycle. In doing so, the dependence of $\left.\frac{da}{dt}\right|_{cycle}$ on crack depth and dwell period must be accounted for. The dwell period affects $\left.\frac{da}{dt}\right|_{hold}$ through the direct integration of the creep crack growth rate [Equation (38)], and also $\left.\frac{da}{dN}\right|_{transient}$ through the possible modification of parameters in the fatigue crack growth law.

5.3 Evaluation of the R5 Procedure

Creep cracking is more of an issue in residual life assessment than design. Neither the ASME Code nor the RCC-MR Code addresses the subject at all. Only R5, which is a guideline, not a code, considers creep cracking explicitly. Therefore, the use of this procedure in the design of HTGR components is limited. However, this procedure presents the use of ductility exhaustion as an alternative to the life fraction rule for calculating the creep component of damage. The use of ductility exhaustion for estimating creep damage had been proposed as an

element of the rules for a possible extension of ASME VIII, Division 2, to elevated temperatures (Corum 1992).

Section 6.3 raises some concern about the use of the linear damage rule to estimate creep/fatigue damage to an HTGR component at elevated temperature. The use of ductility exhaustion instead of the linear damage rule may be more suitable for estimating creep damage in the HTGR materials and should be evaluated for incorporation in Subsection NH.

6.0 Predictive Rules for Creep, Fatigue, and Creep-Fatigue Damage

6.1 "Safety Factors" Two and Twenty on Fatigue Life in Air

The original purpose of adding fatigue as one of the failure modes for which explicit design criteria were provided in Section III was to assure that the reduction of the nominal safety factor for the primary stress limit from four on ultimate tensile strength to three did not result in a decrease in reliability if the vessel was subjected to cyclic stresses. It was originally intended to be a design consideration, not necessarily a valid measure of the eventual operational fatigue life of the vessel, because the manufacturer had no control over how the vessel was operated.

The original fatigue curve for reactor pressure vessel steels in the code was derived by first fitting the then available data to a Manson-Coffin power law, including an endurance limit. A modified Goodman diagram was then used to adjust for mean stress conservatively for stress amplitudes less than the yield stress. The final step was to shift the curve in recognition of the fact that laboratory data were to be applied to actual vessels. This was achieved by applying a factor of two on stress and twenty on cycles, whichever was more conservative. The intent of these factors has been a source of controversy ever since. Some have interpreted these to be factors of safety, but according to one of the original participators in the formulation of the code procedures, "nothing could be further from the truth." Accordingly, it is not to be expected that a vessel will actually operate safely for twenty times its specified life. The factor of twenty applied to cycles was developed to account for real effects. It is the product of the following sub-factors:

Scatter of data (minimum to mean)	2.0
Size effect	2.5
Surface finish, atmosphere, etc.	4.0.

"Atmosphere" was meant to reflect the effects of an industrial atmosphere in comparison to air-conditioned laboratory air, not a specific coolant (reactor water coolant, impure helium, etc.). Since a factor of twenty on cycles has little effect at high cycles, a factor of two on stress was added because at 10,000 cycles (the approximate border between high-cycle and low-cycle fatigue) it gave the same result as a factor of twenty on cycles. Since the adoption of these factors by the ASME Code, they have been accepted by virtually every other nuclear design code.

6.2 Predictive Rules for Creep Damage

Normally creep damage in most materials is a bulk phenomenon, and as such, is not influenced significantly by environment. However, creep tests on Alloy 617 in impure helium show a significant decrease in rupture time and ductility as compared to air. The results have been explained in terms of the lack of formation of a protective oxide scale in the helium environment followed by decarburization of the alloy [Huchtemann 1989, Natesan et al. 2003]. Currently, we do not have prediction models for creep rupture life that can account for such microstructural details. Creep data for code purposes are generally derived from laboratory tests plotted as time to rupture against stress at various temperatures and as functions of environment. Creep rupture data are also sometimes plotted as a Monkman-Grant plot

(Monkman and Grant 1956), which is a power-law relationship between minimum creep rate and time to rupture:

$$\dot{\varepsilon}_m = F \exp\left[-\frac{Q}{R(T+273)}\right] t_R^{-\lambda} \tag{41}$$

where Q is activation energy, R is universal gas constant, t_R is time to rupture, and T is temperature in °C.

If sufficient data are not available, the data are often plotted as stress vs. Larson-Miller parameter (Larson and Miller 1952), which is defined as

$$LMP = (T+273)(C + \log t_R) \tag{42}$$

where T is in °C, t_R is the rupture time, and C is an adjustable parameter. Although other empirical correlations for fitting creep rupture data are available [e.g., Manson-Haferd parameter (Manson and Haferd 1953)], the Larson-Miller parameter generally fits creep data well and has been used by the Materials Properties Council (MPC) to plot creep rupture data of several alloys (Prager, 2002) up to very high temperatures (816°C). Similar Larson-Miller plots can also be generated for time to 1% creep.

Some of the alloys (e.g., Alloy 617) considered for HTGR application display nonclassical creep behavior, i.e., they do not show the usual sequence of primary creep followed by steady-state creep and finally tertiary creep. Instead, creep tends to follow an increasingly steep curve (like tertiary creep) from the beginning of the test (Natesan et al. 2003). This has implication for allowable high-temperature, time-dependent primary stress (S_t), which has been defined for materials with classical creep behavior. A new set of criteria for materials with nonclassical creep behavior will be needed for HTGR application. The Omega method of MPC (Prager, 2002), which has been proposed for modeling tertiary creep behavior of classical creep curves, may be useful for this purpose and should be further investigated.

6.3 Predictive Rules for Fatigue Damage at High Temperature

Fatigue damage at relatively low temperatures, e.g., operating temperatures for light water reactors (LWRs), has been known to depend on environment. At elevated temperatures however, an additional factor is the effect of thermal creep. The original low-temperature design fatigue curves in the ASME Code contained a note that the fatigue curves do not consider the deleterious effects of "unusually corrosive environments." The intent was to distinguish this from the normally expected corrosion effect in vessels, which is accommodated by increasing the thickness to provide a corrosion allowance. That technique does not ameliorate stress corrosion fatigue. The intent was that this effect was to be explicitly considered by the Design Specification. Later editions of Section III have replaced the term "unusually corrosive environments" by "corrosive environments." However, the ASME Code does not give any guidance on how to take the corrosive environmental effect into account.

An example of the importance of environment in fatigue design can be found in the LWR industry. Virtually all the vessels and piping of existing LWRs in the U.S. are designed using ASME Code, Section III, which does not take into account the effects of LWR environments on the fatigue design curves. However, a significant body of laboratory-generated fatigue data in

the LWR environment currently exists. These data indicate that the LWR environment can, under certain conditions, lead to loss of fatigue life that can use up most or all of the factor of twenty on cycles implicit in the fatigue curves currently in the code (Chopra and Shack 1998). Proposed changes in the fatigue design procedure to account for LWR water effects have been submitted to the ASME Code Committee.

A similar situation exists with respect to thermal creep effects at high temperatures. Extensive fatigue tests at elevated temperatures conducted under the US LMFBR program showed that fatigue life of the austenitic stainless steels in high vacuum or air can be drastically reduced by the imposition of a tensile hold period (Majumdar and Maiya 1980). The cyclic life reduction factor can be much greater than the safety factor of twenty that is used in the design fatigue curves. Therefore, the ASME Code developed Subsection NH in which the effect of thermal creep is explicitly taken into account. As mentioned earlier, Subsection NH and most of the other international codes adopted the (cycle fraction/time fraction) linear damage rule for the purpose of evaluating creep-fatigue damage. An alternative version of the linear damage rule uses strain fraction (instead of time fraction) for computing creep damage. For austenitic stainless steels under long tensile hold, the cycle fraction portion of the damage is generally negligible. In these cases, the method reduces to a ductility exhaustion equation, which is mechanistically more attractive than the time fraction approach and has been adopted by the British Code R5 for the austenitic stainless steels. As mentioned earlier, other life-predictive-rules can correlate creep-fatigue test data as well or better than the linear damage rule. These include the Damage Rate Equations (Majumdar and Maiya 1976), Strain Range Partitioning (SRP) Equations (Manson et al. 1971), and Frequency Separation (FS) Equation (Coffin 1971). Various reports have shown that these methods can predict creep-fatigue lives of austenitic stainless steels and Hastelloy-XR better than the linear damage rule (Majumdar, Maiya, and Booker 1981; and Muto, Miyamoto, Nakajima, and Baba 1989). Japanese work has shown that the time-fraction/cycle-fraction linear damage rule or the ductility exhaustion method can predict the life of modified 9Cr-1Mo steel under tensile hold but not under compressive hold (Aoto et al. 1994). No significant new predictive model for failure of initially uncracked specimens has been proposed in recent years, although significant advances have been made in the area of crack propagation at high temperatures.

Damage Rate Equations are a set of crack and intergranular cavity growth rate (or damage rate) equations in terms of the inelastic strain rate, which accounts for the greater damage caused by lower inelastic strain rates (i.e., creep-like) than higher inelastic strain rates (i.e., plasticity-like) in a continuous manner. Since this method does not distinguish between plastic and creep strains, it can be easily integrated with the unified constitutive equations that are necessary at high temperatures. Further, since this method takes into account the increasing damage accumulation with decreasing strain rate (i.e., longer hold times), it should be reliable for extrapolation from the database. On the other hand, the SRP equations divide the inelastic strain into plastic and creep components in the classical sense and are, therefore, incompatible with the unified constitutive equations. The FS equation is expressed in terms of the frequency of loading and basically attributes most of the creep-fatigue damage to environmental effects. None of these alternative life predictive models has been applied to the creep-fatigue database available for most of the materials being considered for HTGR application.

At high temperatures, creep, fatigue, and environment interact. For example, in addition to its fatigue life (without hold time) being decreased with decreasing strain rate, the fatigue life

of austenitic stainless steel at a given strain rate is increased significantly in high purity sodium or high vacuum when compared to that in air. Fatigue tests (without hold) conducted on Alloy 617 and Hastelloy X at high temperatures in impure helium environment show no reduction in fatigue life compared to that in air. Generally, in the absence of hold periods, fatigue lives of the alloys tested in impure helium environment do not show any deleterious effect compared to those in air. However, at high temperatures, cyclic fatigue lives (without hold) of most alloys decrease with decreasing strain rate (Majumdar, Maiya, and Booker 1981). In materials (e.g., austenitic stainless steels, modified 9Cr-1Mo steel) that are prone to grain boundary cavitation at high temperature, environment plays a relatively minor role when they are subjected to cycles with long tensile hold time. On the other hand, environment can play a significant role in the same materials under cycles with compressive hold period. For materials that are not prone to caviation (e.g., 2-1/4Cr-1Mo steel tested at low strain range), compressive hold can be more damaging than tensile hold (Majumdar, Maiya, and Booker 1981).

At a minimum, two types of models are needed for life prediction of high-temperature fatigue. First, for materials that sustain bulk creep damage under tensile holds, either the ductility exhaustion (or the linear damage rule) equation or the alternative life prediction methods discussed above can be used. The continuum damage mechanics approach can also be utilized for this type of materials. Second, for materials that do not experience bulk creep damage but sustain surface cracking due to environmental (e.g., oxidation or decarburization) effect, a different life predictive method for crack initiation is needed. The available models in this area are rather limited. A life predictive model for 2-1/4Cr-1Mo steel was presented by Majumdar, Maiya, and Booker (1981), who combined an oxide-cracking model (Manning and Metcalfe, 1977) with the damage rate equation for crack growth. Challenger, Miller, and Brinkman (1981) also proposed an oxide-cracking model for the same material. These and other types of environmental fatigue damage models should be explored further for application to HTGRs.

7.0 Findings

The objective of the task is to review and evaluate currently available national and international codes and procedures to be used in design of high-temperature gas-cooled reactors (HTGRs) including, but not limited to, the Pebble Bed Modular Reactor (PBR) and the Gas Turbine-Modular Helium Reactor (GT-MHR). The approach includes evaluation of the applicability of the codes, standards, and procedures to the materials that have been used or recommended for HTGRs, taking into account the HTGR operating environments. The following codes, code cases, and procedure are identified as applicable to high-temperature design:

ASME B&PV Code, Section III, Subsection NB, Class 1 Components,

ASME B&PV Code, Section III, Subsection NH, Class 1 Components in Elevated Temperature Service,

ASME B&PV Code Case N-499-1, Use of SA-533 Grade B, Class 1 Plate and SA-508 Class 3 Forgings and Their Weldments for Limited Elevated Temperature Service,

ASME B&PV Code Case N-201-4, Class CS Components in Elevated Temperature Service,

Draft ASME B&PV Code Case for Alloy 617 (was being developed by the Task Group on Very-High Temperature Design),

RCC-MR, Design and Construction Rules for Mechanical Components of FBR Nuclear Islands (French Code), and

Procedure R5, Assessment Procedures for the High Temperature Response of Structures (British Procedure).

These codes, code cases, and procedure are reviewed and evaluated for their applicability to the design of HTGR components. The findings of the evaluation are as follows:

- The maximum temperature permitted by the codes and code cases for the materials acceptable for HTGR components is lower (760°C) than the maximum temperature (≥850°C) that these components may experience during operation. The scope of the code and code cases needs to be expanded to include the materials with allowable temperatures of 850°C and higher.
- The codes and code cases do not provide specific guidelines for environmental effects, especially the effect of impure helium on the high temperature behavior (e.g., creep and creep-fatigue) of the materials considered. The needed data on environmental effects should be collected and/or generated, so that the specific guidelines for these effects can be developed.
- One of the main difficulties of using the reviewed codes and code cases to the design of HTGR components is the rather limited choice of materials.
- Austenitic stainless steels (Types 304 and 316 SS) have commonly been used for high-temperature steam application due to their excellent strength retention at high temperatures. However, sufficient database is not available for the use of these alloys at temperatures of 600°C and higher in an impure helium environment of HTGRs. Furthermore, the austenitic stainless steels exhibit high thermal expansion rates and low thermal conductivity. This results in the development of high thermally induced stresses during heating and cooling, which can cause thermal fatigue and creep.

- The review has identified only one material, Alloy 617, that has allowable temperature [982°C (1800°F)] greater than 850°C. Draft ASME Code Case for Alloy 617 provides design rules for very-high-temperature reactors such as GT-MHR. The draft code case is based on limited database and minimal service experience. Further development of the draft code case is needed before reliable application of the alloy. Recommendations for further development are presented below in three categories:

  Actions Required to Complete the Draft Case:

  - Alloy 617 must be added to the low-temperature rules of Section III.
  - Weldment stress rupture factors must be added.
  - Thermal expansion coefficient must be added.
  - Additional isochronous stress-strain curves at 427°C to 649°C must be added.

  Material Data Needs

  - Weldment fatigue data.
  - More complete creep-fatigue database.
  - The synergistic effects of aging, environment, loading, and temperature.
  - The effects of aging on toughness of materials.

  Structural Design Methodology Needs

  - Unified constitutive model is needed for developing isochronous stress strain curves.
  - Some very-high-temperature, time-dependent tests of Alloy 617 structural models are needed to (1) provide better understanding of structural behavior and failure modes, and (2) validate inelastic analysis methods and failure modes.
  - Simplified ratcheting evaluation procedures need to be developed for temperatures above 649°C.
  - The use of linear damage fractions as the basis of the creep-fatigue rules is probably the biggest shortcoming of the draft case. A basic effort is needed to identify and experimentally validate a more fitting damage theory.
- The fatigue and creep-fatigue evaluation procedures in the codes and code cases reviewed do not account for environmental effects. High-temperature fatigue life may be influenced more by environment than by creep damage for materials other than austenitic stainless steels. Therefore, extrapolation of creep-fatigue life beyond the database may be less of a problem for stainless steels than the ferritic steels. Carburization or decarburization in impure gaseous He environment may have an effect on high-temperature fatigue life, which needs to be explored by tests.
- The use of the bilinear creep and fatigue damage summation rule may not be applicable to all materials. The R5 Procedure uses ductility exhaustion as an alternative to linear damage rule for calculating the creep component of the damage in austenitic stainless steels. The possibility for the use of ductility exhaustion or other mechanistically based life-predictive methods for estimating creep-fatigue life of the HTGR materials should be evaluated.

References

Ainsworth, R. A., M. B. Ruggles, and Y. Takahashi 1992. "Flaw Assessment Procedure for High-Temperature Reactor Components," Journal of Pressure Vessel Technology, Transaction of ASME, 114, pp. 166-170.

Aoto, K., R. Komine, F. Ueno, H. Kawasaki, and Y. Wada 1994. "Creep-Fatigue Evaluation of Normalized and Tempered 9Cr-1Mo," Nucl. Eng. and Design, 153, pp. 97-110.

ASME 2001. *ASME Boiler and Pressure Vessel Code, Section III,* the American Society of Mechanical Engineers, New York.

Autrusson, B., 1988. "Comparison of Code Case N47-23 and RCC-MR Rules for the Prevention of Ratcheting in Case of Significant Creep," Rapport DEMT 88/003, Commissariat a l'Energie Atomique.

Boyer, V. S., et al., 1974. "Fulton Station HTGR," Nucl. Engg. Intl. August, pp. 635-659.

Brey, H. L. 2000. "Developmental History of the Gas Turbine Modular High Temperature Reactor," IAEA-TECDOC--1238, presented at the IAEA Technical Committee Meeting on *Gas Turbine Power Conversion for Modular HTGRs,* held 14-16 November 2000, Palo Alto, California.

Buckthorpe, D., et al., 2002. "Investigation of High Temperature Reactor (HTR) Materials," presented at the 2nd Information Meeting on High Temperature Reactor Materials (HTR), NNC Limited.

Challenger, K., A. K. Miller, and C. R. Brinkman, 1981. "An Explanation for the Effects of Hold Periods on the Elevated Temperature Fatigue Behavior of 2-1/4Cr-1Mo steel," J. Eng. Mater. Techno. 103.

Chellapandi, P., R. Ramesh, S. C. Chetal, and S. B. Bhoje 1996. "Application of Chaboche Viscoplastic Theory for Predicting the Cyclic Behavior of Modified 9Cr-1Mo (T91)," *Creep-Fatigue Damage Rules for Advanced Fast Reactor Design*, IAEA-TELDOC—933, International Atomic Energy Agency, Vienna, Austria.

Chopra, O. K., and W. J. Shack 1998. *Effects of LWR Coolant Environments on Fatigue Design Curves of Carbon and Low Alloy Steels*, NUREG/CR-6583.

Coffin, L. F., 1971. "The Effect of Frequency on the Cyclic Strain and Low Cycle Fatigue Behavior of Cast Udimet 500 At Elevated Temperature," Met. Trans., 2, p. 3105.

Cooper, W. E., 1992. "The Initial Scope and Intent of the Section III Fatigue Design Procedure," in *Technical Information from Workshop on Cyclic Life and Environmental Effects in Nuclear Applications,* Clearwater, Florida, January 20–21, 1992, Welding Research Council, Inc., New York.

Corum, J. M., and J. J. Blass 1991. "Rules for Design of Alloy 617 Nuclear Components to Very High Temperatures," Fatigue, Fracture, and Risk, PVP-Vol. 215, American Society of Mechanical Engineers, New York.

Corum, J. M., 1992. Revised Creep-Fatigue and Creep Damage Evaluation Procedure for Section VIII/Div. 2.

EPRI 2002. *Evaluation of Materials Issues in the PBMR and GT-MHR*, draft document, October 17, 2002, Electric Power Research Institute, Palo Alto, CA.

Goodall, I. W., and R. A. Ainsworth, 1991. "R5: An Assessment Procedure for the High Temperature Response of Structures," *11th International Conference on Structural Mechanics in Reactor Technology,* Tokyo Atomic Energy Society of Japan, Tokyo, Japan, pp. 91-96.

Huchtemann, B., 1989. "The Effect of Alloy Chemistry on Creep Behaviour in a Helium Environment with Low Oxygen Partial Pressure," Materials Science and Engineering, A121, pp. 623-626.

IAEA 2001. "Chapter 4: Review of the Gas Turbine-Modular Helium Reactor (GT-MHR) Plant,"*Current Status and Future Development of Modular High Temperature Gas Cooled Reactor Technology,* IAEA-TECDOC-1198, International Atomic Energy Agency, Vienna, Austria, pp. 69-113.

Jaske, C. E., and W. J. O'Donnell 1977. "Fatigue Design Criteria for Pressure Vessel Alloys," Trans. ASME J. Pressure Vessel Technology, 99, pp. 584–592.

Kiryushin, A. I., et al., 1997. "Project of the GT-MHR High-Temperature Helium Reactor with Gas Turbine," Nucl. Eng. And Design, 173, pp. 119-129.

LaBar, M. P., 2002. "The Gas Turbine – Modular Helium Reactor: A Promising Option for Near Term Deployment," GA-A23952, General Atomics, San Diego, CA.

Langer, B. F., 1962. "Design of Pressure Vessels for Low–Cycle Fatigue," ASME J. Basic Eng. 84, pp. 389–402.

Larson, F. R., and J. Miller 1952. "A Time-Temperature Relationship for Rupture and Creep Stresses," *Trans. ASME,* 74, p. 765.

Majumdar, S. and P. S. Maiya 1976. *A Unified and Mechanistic Approach to Creep-Fatigue Damage*, ANL-76-58, Argonne National Laboratory.

Majumdar, S. and P. S. Maiya 1980. "A Mechanistic Model for Time-Dependent Fatigue," J. Eng. Mat. Tech., 102, pp. 159-167.

Majumdar, S., P. S. Maiya, and M. K. Booker 1981. *A Review of Time-Dependent Fatigue Behavior and Life Prediction for Type 304 Stainless Steel and 2-1/4Cr-1Mo Steel,* ANL-81-20, Argonne National Laboratory.

Manjoine, M. J., and R. L. Johnson 1986. "Development of Fatigue Design Curves for Ferritic Steels up to 700°F (371°C)," *Symposium on ASME Codes and Recent Advances in PVP and Valve Technology Including a Survey of Operations Research Methods in Engineering,* PVP-Vol. 109, American Society of Mechanical Engineers, New York, pp. 77-85.

Manning, M. I., and E. Metcalfe 1977. "Oxidation of Ferritic Steels in Steam," in Int. Conf. on Ferritic Steels for Fast Breeder Reactor Steam Generators, British Nuclear Energy Society, London, Paper No. 63.

Manson, S. S., 1966. *Thermal Stress and Low Cycle Fatigue*, McGraw-Hill, New York, pp. 165-170.

Manson, S. S., and A. M. Haferd 1953. "A Linear Time-Temperature Relation for Extrapolation of Creep and Stress Rupture Data," NASA Technical Note 2890, National Aeronautic and Space Administration.

Manson, S. S., G. R. Halford, and M. H. Hirschberg 1971. "Creep-Fatigue Analysis by Strain Range Partitioning," in *Design for Elevated Temperature Environment*, American Society of Mechanical Engineers, New York, pp. 12-28.

Monkman, F. C., and N. J. Grant 1956. "An Empirical Relationship Between Rupture Life and Minimum Creep Rate in Creep Rupture Tests," Proc. ASTM, 56, p. 593.

Muto, Y., et al., 2000. "Selection of JAERI's HTGR-GT Concept," IAEA-TECDOC--1238, presented at the IAEA Technical Committee Meeting on *Gas Turbine Power Conversion for Modular HTGRs*, held 14-16 November 2000, Palo Alto, CA.

Muto, Y., Y. Miyamoto, H. Nakajima, and O. Baba 1989. "The Present Status of Research and Development Works for the Preparation of the High Temperature Design Code," Proc. Workshop on Structural Design Criteria for HTR, Edited by G. Breitbach et al., Julich, Germany.

Natesan, K., A. Purohit, and S. W. Tam 2003. *Materials Behavior in HTGR Environments*, Argonne National Laboratory Report, to be published.

Nickel, H., 1989. "Present Status of the High Temperature Reactor in the Federal Republic of Germany," in Proceedings of the Workshop on Structural Design Criteria for HTR, Julich, 31 January–1 February, 1989, Jul-Conf-71, Breitbach, G., F. Schubert, and H. Nickel (Eds.), pp. 59-77.

Penny, R. K., and D. L. Marriott 1995. *Design for Creep*, Chapman & Hill, London.

Prager, M., 1996. "Proposed Implementation of Criteria for Assignment of Allowable Stresses High in the Creep Range," in Structural Integrity NDE Risk and Material Performance for Petroleum, Process and Power, PVP-Vol. 336, American Society of Mechanical Engineers, New York, pp. 273-293.

Robinson, D. N., 1984. "Constitutive Relationships for Anisotropic High-Temperature Alloys," Nuclear Engineering and Design, 83, pp. 389-396.

Shenoy, A. S., and W. S. Betts 1988. "Design Requirements for High Temperature Metallic Component Materials in the US Modular HTGR," Proceedings of a Specialists Meeting Held in Cracow, 20-23 June 1988, pp. 34-42

Strizak, J. P., C. R. Brinkman, M. K. Booker, and P. L. Rittenhouse 1982. *The Influence of Temperature, Environment, and Thermal Aging on the Continuous Cycle Fatigue Behavior of Hastelloy X and Inconel 617*, ORNL/TM-8130, Oak Ridge National Laboratory, Oak Ridge, Tennessee.

Yukawa, S., 1991. "Elevated Temperature Fatigue Design Curves for Ni-Cr-Co-Mo Alloy 617," First JSME/ASME Joint International Conf. on Nuclear Engineering, Tokyo, Japan, Nov. 4-7, 1991.